# Government Polytechnic, Sonepur

# LECTURE NOTE

## SUBJECT NAME- MATERIAL TESTING

**PREPARED BY- ARPITA JENA**
**(PTGF)**

# THE HARDNESS TEST

## 9-1 INTRODUCTION

- The hardness of a material is a poorly defined term which has many meanings depending upon the experience of the person involved.
- In general, hardness usually implies a resistance to deformation, and for metals the property is a measure of their resistance to permanent or plastic deformation.
- To a person concerned with the mechanics of materials testing, hardness is most likely to mean the resistance to indentation, and to the design engineer it often means an easily measured and specified quantity which indicates something about the strength and heat treatment of the metal.
- There are three general types of hardness measurements depending on the manner in which the test is conducted. These are

(1) **Scratch hardness,**

(2) **Indentation hardness, and**

(3) **Rebound, or Dynamic, hardness.**

- Only indentation hardness is of major engineering interest for metals.
- Scratch hardness is of primary interest to mineralogists.
- With this measure of hardness, various minerals and other materials are rated on their ability to scratch one another.
- Scratch hardness is measured according to the Mohs' scale. This consists of 10 standard minerals arranged in the order of their ability to be scratched.
- The softest mineral in this scale is talc (scratch hardness 1), while diamond has a hardness of 10. A fingernail has a value of about 2, annealed copper has a value of 3, and martensite a hardness of 7.
- The Mohs' scale is not well suited for metals since the intervals are not widely spaced in the high-hardness range. Most hard metals fall in the Mohs' hardness range of 4 to 8.
- A different type of scratch-hardness test1 measures the depth or width of a scratch made by drawing a diamond stylus across the surface under a definite load. This is a useful tool for measuring the relative hardness of micro constituents, but it does not lend itself to high reproducibility or extreme accuracy.

- In dynamic-hardness measurements the indenter is usually dropped onto the metal surface, and the hardness is expressed as the energy of impact. The Shore scleroscope, which is the commonest example of a dynamic-hardness tester, measures the hardness in terms of the height of rebound of the indenter.

## 9-2 BRINELL HARDNESS

- The first widely accepted and standardized indentation-hardness test was proposed by J. A. Brinell in 1900.
- The Brinell hardness test consists in indenting the metal surface with a 10-mmdiameter steel ball at a load of 3,000 kg. For soft metals the load is reduced to 500 kg to avoid too deep an impression, and for very hard metals a tungsten carbide ball is used to minimize distortion of the indenter.
- The load is applied for a standard time, usually 30 s, and the diameter of the indentation is measured with a low-power microscope after removal of the load.
- The average of two readings of the diameter of the impression at right angles should be made. The surface on which the indentation is made should be relatively smooth and free from dirt or scale.
- The Brinell hardness number (BHN) is expressed as the load P divided by the surface area of the indentation.

This is expressed by the formula

$$\text{BHN} = \frac{P}{(\pi D/2)\left(D - \sqrt{D^2 - d^2}\right)} = \frac{P}{\pi D t} \qquad (9.1)$$

Where,

P = applied load, kg D =
diameter of ball, mm d =
diameter of indentation, mm t =
depth of the impression, mm

- It will be noticed that the units of the BHN are kilograms per square millimetre (1 kgf mm $^{-}$2 = 9.8 MPa).
- However, the BHN is not a satisfactory physical concept since Eq. (9-1) does not give the mean pressure over the surface of the indentation.

From Fig. 9-1 it can be seen that d = D Sin ∅. Substitution into Eq. (9-1) gives an alternate expression for Brinell hardness number.

$$\text{BHN} = \frac{P}{(\pi/2) D^2 (1 - \cos \phi)} \tag{9.2}$$

- In order to obtain the same BHN with a nonstandard load or ball diameter it is necessary to produce geometrically similar indentations.
- Geometric similitude is achieved so long as the included angle 2∅ remains constant. Equation (9-2) shows that for∅ and BHN to remain constant the load and ball diameter must be varied in the ratio

$$\frac{P_1}{D_1^2} = \frac{P_2}{D_2^2} = \frac{P_3}{D_3^2} \tag{9.3}$$

- Unless precautions are taken to maintain P/D2 constant, which may be experimentally inconvenient, the BHN generally will vary with load.
- Over a range of loads the BHN reaches a maximum at some intermediate load. Therefore, it is not possible to cover with a single load the entire range of hardnesses encountered in commercial metals.
- The relatively large size of the Brinell impression may be an advantage in averaging out local heterogeneities.
- Moreover, the Brinell test is less influenced by surface scratches and roughness than other hardness tests.
- On the other hand, the large size of the Brinell impression may preclude the use of this test with small objects or in critically stressed parts where the indentation could be a potential site of failure.

## 9-3 MEYER HARDNESS

- Meyer suggested that a more rational definition of hardness than that proposed by Brinell would be one based on the projected area of the impression rather than the surface area.
- The mean pressure between the surface of the indenter and the indentation is equal to the load divided by the projected area of the indentation.

$$p_m = \frac{P}{\pi r^2}$$

- Meyer proposed that this mean pressure should be taken as the measure of hardness. It is referred to as the Meyer hardness.

$$\text{Meyer hardness} = \frac{4P}{\pi d^2} \qquad (9.4)$$

- Like the Brinell hardness, Meyer hardness has units of kilograms per square millimetre.
- The Meyer hardness is less sensitive to the applied load than the Brinell hardness.
- For a cold-worked material the Meyer hardness is essentially constant and independent of load, while the Brinell hardness decreases as the load increases.
- For an annealed metal the Meyer hardness increases continuously with the load because of strain hardening produced by the indentation.
- The Brinell hardness, however, first increases with load and then decreases for still higher loads.
- The Meyer hardness is a more fundamental measure of indentation hardness; yet it is rarely used for practical hardness measurements.

Meyer proposed an empirical relation between the load and the size of the indentation. This relationship is usually called Meyer's law

$$P = kd^{n'} \qquad (9.5)$$

Where,

P= applied load, kg d= diameter of indentation, mm n'= a material constant related to strain hardening of metal k = a material constant expressing resistance of metal to penetration

## 9-4 RELATIONSHIP BETWEEN HARDNESS AND THE FLOW CURVE

- Tabor has suggested a method by which the plastic region of the true stress-true-strain curve may be determined from indentation hardness measurements.

The method is based on the fact that there is a similarity in the shape of the low curve and the curve obtained when the Meyer hardness is measured on a number of specimens subjected to increasing amounts of plastic strain.

- The method is basically empirical, since the complex stress distribution at the hardness indentation precludes a straightforward relationship with the stress distribution  in the tension or compression test.
- However, the method has been shown to give good agreement for several metals, and thus should be of interest as a means of obtaining low data in situations where it is not possible to measure tensile properties.
- The true stress (low stress) is obtained from Eq. (9-6), where $\sigma_0$ is to be considered the flow stress at a given value of true strain. From a study of the deformation at indentations, Tabor concluded that the true strain was proportional to the ratio d/D and could be expressed as

$$\varepsilon = 0.2\frac{d}{D} \qquad (9.7)$$

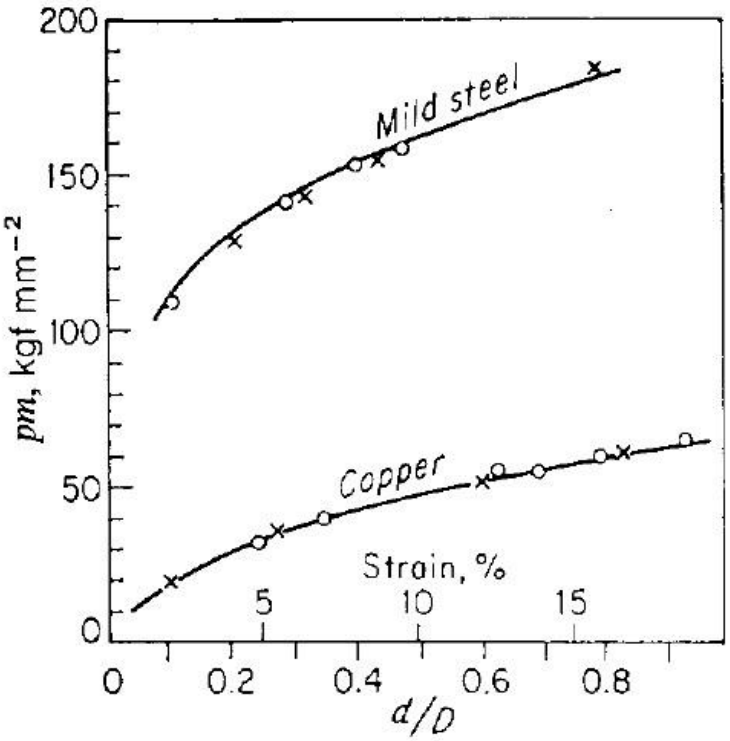


Figure 9-3 Comparison of low curve determined from hardness measurements (circles and crosses with low curve determined from compression test (solid lines). (100 kgf $mm^{-2}$ = 981 MPa.)

There is a very useful engineering correlation between the Brinell hardness and the ultimate tensile strength of heat-treated plain-carbon and medium-alloy steels (see Fig. 8-28).

Ultimate tensile strength, in MPa = 3.4(BHN)

## 9-5 VICKERS HARDNESS

- The Vickers hardness test uses a square-base diamond pyramid as the indenter.
- The included angle between opposite faces of the pyramid is 136°. This angle was chosen because it approximates the most desirable ratio of indentation diameter to ball diameter in the Brinell hardness test.
- Because of the shape of the indenter, this is frequently called the diamond-pyramid hardness test.
- The diamond-pyramid hardness number (DPH), or Vickers hardness number (VHN, or VPH), is defined as the load divided by the surface area of the indentation.
- In practice, this area is calculated from microscopic measurements of the lengths of the diagonals of the impression.

The DPH may be determined from the following equation

$$\text{DPH} = \frac{2P\sin(\theta/2)}{L^2} = \frac{1.854P}{L^2} \qquad (9.9)$$

Where,

P= applied load, kg

L = average length of diagonals, mm

$\theta$= angle between opposite faces of diamond =136 $^0$

- The Vickers hardness test has received fairly wide acceptance for research work because it provides a continuous scale of hardness, for a given load, from very soft metals with a DPH of 5 to extremely hard materials with a DPH of 1,500.
- With the Rockwell hardness test, described in Sec. 9-7, or the Brinell hardness test, it is usually necessary to change either the load or the indenter at some point in the hardness scale, so that measurements at one extreme of the scale cannot be strictly compared with those at the other end.

Because the impressions made by the pyramid indenter are geometrically similar no matter what their size, the DPH should be independent of load.

- This is generally found to be the case, except at very light loads. The loads ordinarily used with this test range from 1 to 120 kg, depending on the hardness of the metal to be tested.
- Inspite of these advantages, the Vickers hardness test has not been widely accepted for routine testing because it is slow, requires careful surface preparation of the specimen, and allows greater chance for personal error in the determination of the diagonal length.

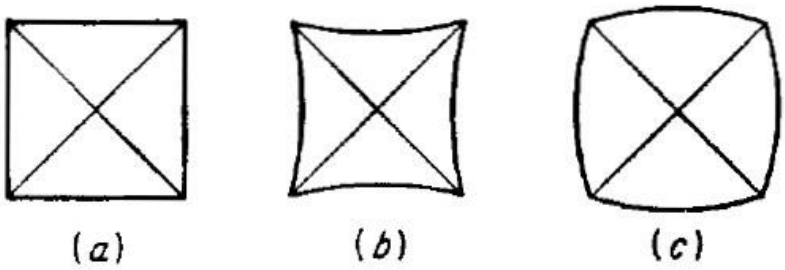


Figure 9-4 Types of diamond-pyramid indentations. (a) Perfect indentation; (b) pincushion indentation due to sinking in; (c) barrelled indentation due to ridging.

- A perfect indentation made with a perfect diamond-pyramid indenter would be a square.
- However, anomalies corresponding to those described earlier for Brinell impressions are frequently observed with a pyramid indenter (Fig. 9-4).
- The pincushion indentation in Fig. 9-4b is the result of sinking in of the metal around the flat faces of the pyramid.
- This condition is observed with annealed metals and results in an overestimate of the diagonal length.
- The barrel-shaped indentation in Fig. 9-4c is found in cold-worked metals. It results from ridging or piling up of the metal around the faces of the indenter.
- The diagonal measurement in this case produces a low value of the contact area so that the hardness numbers are erroneously high. Empirical corrections for this effect have been proposed.

## 9-6 ROCKWELL HARDNESS TEST

- The most widely used hardness test in the United States is the Rockwell hardness test.

Its general acceptance is due to its speed, freedom from personal error, ability to distinguish small hardness differences in hardened steel, and the small size of the indentation, so that finished heat-treated parts can be tested without damage.

- This test utilizes the depth of indentation, under constant load, as a measure of hardness.
- A minor load of 10 kg is first applied to seat the specimen.
- This minimizes the amount of surface preparation needed and reduces the tendency for ridging or sinking in by the indenter.
- The major load is then applied, and the depth of indentation is automatically recorded on a dial gage in terms of arbitrary hardness numbers.
- The dial contains 100 divisions, each division representing a penetration of 0.002 mm.
- The dial is reversed so that a high hardness, which corresponds to a small penetration, results, in a high hardness number.
- This is in agreement with the other hardness numbers described previously, but unlike the Brinell and Vickers hardness designations, which have units of kilograms per square millimetre (kgf $mm^{-2}$), the Rockwell hardness numbers. are purely arbitrary.
- One combination of load and indenter will not produce satisfactory results for materials with a wide range of hardness.
- A 120° diamond cone with a slightly rounded point, called a Brale indenter, and 1.6- and 3.2 mm diameters steel balls are generally used as indenters.
- Major loads of 60, 100, and 150 kg are used.
- Since the Rockwell hardness is dependent on the load and indenter, it is necessary to specify the combination which is used.
- This is done by prefixing the hardness number with a letter indicating the particular combination of load and indenter for the hardness scale employed.
- A Rockwell hardness number without the letter prefix is meaningless.
- Hardened steel is tested on the C scale with the diamond indenter and a 150-kg major load.
- The useful range for this scale is from about $R_c$ 20 to $R_c$ 70.

- Softer materials are usually tested on the B scale with a 1.6mm-diameter steel ball and a 100 kg major load.
- The range of this scale is from $R_B$ 0 to $R_B$ 100.

The A scale (diamond penetrator, 60-kg major load) provides the most extended Rockwell hardness scale, which is usable for materials from annealed brass to cemented carbides.

- Many other scales are available for special purposes.

The Rockwell hardness test is a very useful and reproducible one provided that a number of simple precautions are observed. Most of the points listed below apply equally well to the other hardness tests:

1. The indenter and anvil should be clean and well seated.
2. The surface to be tested should be clean and dry, smooth, and free from oxide. A roughground surface is usually adequate for the Rockwell test.
3. The surface should be flat and perpendicular to the indenter.
4. Tests on cylindrical surfaces will give low readings, the error depending on the curvature, load, indenter, and hardness of the material. Theoretical and empirical corrections for this effect have been published.
5. The thickness of the specimen should be such that a mark or bulge is not produced on the reverse side of the piece. It is recommended that the thickness be at least 10 times the depth of the indentation. Tests should be made on only a single thickness of material.
6. The spacing between indentations should be three to five times the diameter of the indentation.
7. The speed of application of the load should be standardized. This is done by adjusting the dashpot on the Rockwell tester. Variations in hardness can be appreciable in very soft materials unless the rate of load application is carefully controlled. For such materials the operating handle of the Rockwell tester should be brought back as soon as the major load has been fully applied.

## 9-7 MICROHARDNESS TESTS

- Many metallurgical problems require the determination of hardness over very small areas.
- The measurement of the hardness gradient at a carburized surface, the determination of the hardness of individual constituents of a microstructure, or the checking of the hardness of a delicate watch gear might be typical problems.

The use of a scratch-hardness test for these purposes was mentioned earlier, but an indentation-hardness test has been found to be more useful.

- The development of the Knoop indenter by the National Bureau of Standards and the introduction of the Tukon tester for the controlled application of loads down to 25 g have made micro hardness testing a routine laboratory procedure
- The Knoop indenter is a diamond ground to a pyramidal form that produces a diamondshaped indentation with the long and short diagonals in the approximate ratio of 7 :1 resulting in a state of plane strain in the deformed region.
- The Knoop hardness number (KHN) is the applied load divided by the unrecovered projected area of the indentation.

$$\mathrm{KHN} = \frac{P}{A_p} = \frac{P}{L^2 C} \qquad (9.10)$$

Where,

P = applied load, kg

$A_p$ = unrecovered projected area of indentation, $mm^2$

L = length of long diagonal, mm

C= a constant for each indenter supplied by manufacturer

- The special shape of the Knoop indenter makes it possible to place indentations much closer together than with a square Vickers indentation, e.g., to measure a steep hardness gradient.
- Its other advantage is that for a given long diagonal length the depth and area of the Knoop indentation are only about 15 percent of what they would be for a Vickers indentation with the same diagonal length.

- This is particularly useful when measuring the hardness of a thin layer (such as an
- electroplated layer), or when testing brittle materials where the tendency for fracture is proportional to the volume of stressed material.
- The low load used with micro hardness tests requires that extreme care be taken in all stages of testing.
- The surface of the specimen must be carefully prepared.
- Metallographic polishing is usually required.

Work hardening of the surface during polishing can influence the results.

- The long diagonal of the Knoop impression is essentially unaffected by elastic recovery for loads greater than about 300 g.
- However, for lighter loads the small amount of elastic recovery becomes appreciable. Further, with the very small indentations produced at light loads the error in locating the actual ends of the indentation become greater.
- Both these factors have the effect of giving a high hardness reading, so that it is usually observed that the Knoop hardness number increases as the load is decreased below about 300 g.

## 9-10 HARDNESS AT ELEVATED TEMPERATURES

In an extensive review of hardness data at different temperatures Westbrook showed that the temperature dependence of hardness could be expressed by

$$H = Ae^{-BT} \tag{9.11}$$

Where,

H = hardness, kgf $mm^{-2}$

T = test temperature, K

A, B = constants

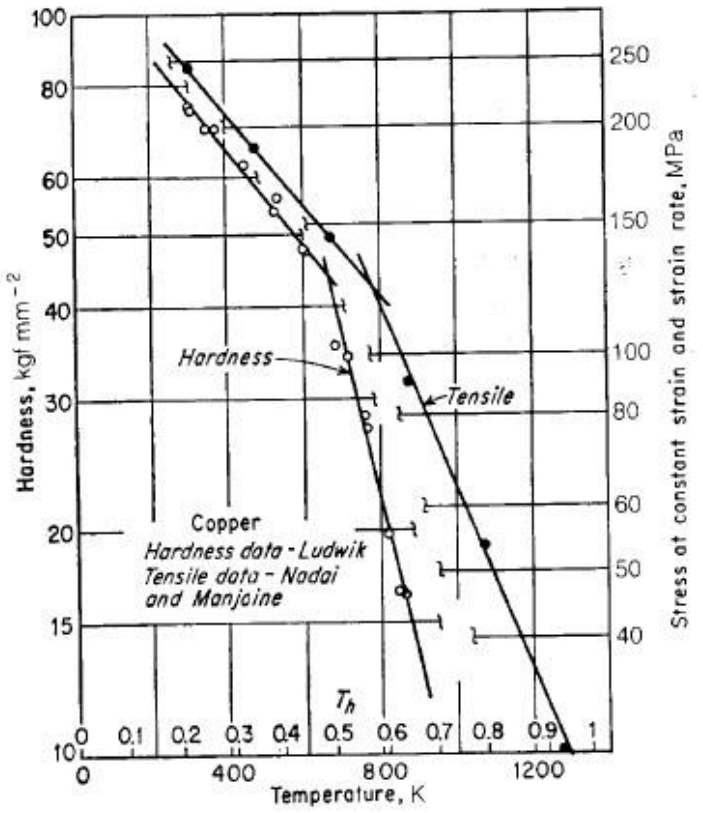


Figure 9-5 Temperature dependence of the hardness of copper

- Plots of log H versus temperature for pure metals generally yield two straight lines of different slope.
- The change in slope occurs at a temperature which is about one-half the melting point of the metal being tested.
- Similar behavior is found in plots of the logarithm of the tensile strength against temperature. Figure 9-5 shows this behavior for copper. It is likely that this change in slope is due to a change in the deformation mechanism at higher temperature.
- The constant A derived from the low-temperature branch of the curve can be considered to be the intrinsic hardness of the metal, that is, H at 0 K.
- This value would be expected to be a measure of the inherent strength of the binding forces of the lattice.
- Westbrook correlated values of A for different metals with the heat content of the liquid metal at the melting point and with the melting point.
- This correlation was sensitive to crystal structure.
- The constant B, derived from the slope of the curve, is the temperature coefficient of hardness.

This constant was related in a rather complex way to the rate of change of heat content with increasing temperature.

- With these correlations it is possible to calculate fairly well the hardness of a pure metal as a function of temperature up to about one-half its melting point.
- Hardness measurements as a function of temperature will show an abrupt change at the temperature at which an allotropic transformation occurs.
- Hot hardness tests on Co, Fe, Ti, U, and Zr have shown that the body-cantered cubic lattice is always the softer structure when it is involved in an allotropic transformation.
- The face-cantered cubic and hexagonal close-packed lattices have approximately the same strength, while highly complex crystal structures give even higher hardness.

These results are in agreement with the fact that austenitic iron-based alloys have better high-temperature strength than ferritic alloys.

# THE TENSION TEST

## 8-1 ENGINEERING STRESS-STRAIN CURVE

- The engineering tension test is widely used to provide basic design information on the strength of materials and as an acceptance test for the specification of materials.
- In the tension test a specimen is subjected to a continually increasing uniaxial tensile force while simultaneous observations are made of the elongation of the specimen.
- An engineering stress-strain curve is constructed from the load-elongation measurements (Fig. 8-1).
- The stress used in this stress-strain curve is the average longitudinal stress in the tensile specimen. It is obtained by dividing the load by the original area of the cross section of the specimen.

$$s = \frac{P}{A_0} \qquad (8.1)$$

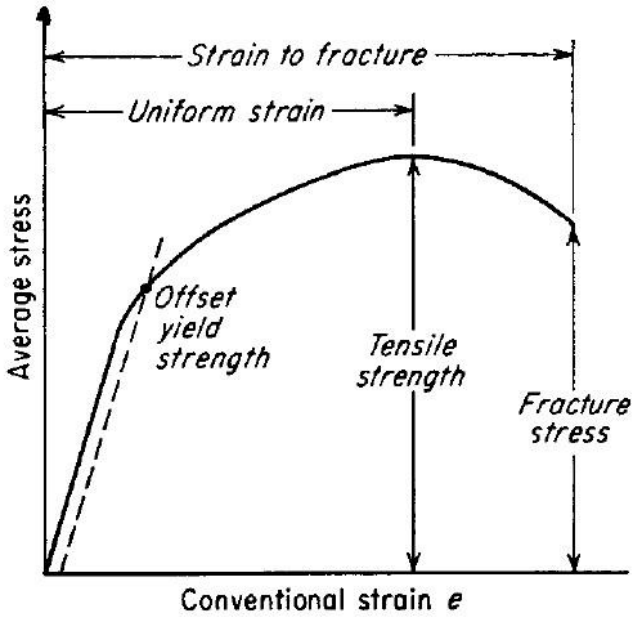


Figure 8-1 The engineering stress-strain curve.

- The strain used for the engineering stress-strain curve is the average linear strain, which is obtained by dividing the elongation of the gage length of the specimen, δ, by its original length.

$$e = \frac{\delta}{L_0} = \frac{\Delta L}{L} = \frac{L - L_0}{L_0} \qquad (8.2)$$

- Since both the stress and the strain are obtained by dividing the load and elongation by constant factors, the load-elongation curve will have the same shape as the engineering stress-strain curve. The two curves are frequently used interchangeably.
- The shape and magnitude of the stress-strain curve of a metal will depend on its composition, heat treatment, prior history of plastic deformation, and the strain rate, temperature, and state of stress imposed during the testing.
- The parameters which are used to describe the stress-strain curve of a metal are the tensile strength, yield strength or yield point, percent elongation, and reduction of area. The first two are strength parameters; the last two indicate ductility.
- The general shape of the engineering stress-strain curve (Fig. 8-1) requires further explanation.
- In the elastic region stress is linearly proportional to strain. When the load exceeds a value corresponding to the yield strength, the specimen undergoes gross plastic deformation.
- It is permanently deformed if the load is released to zero. The stress to produce continued plastic deformation increases with increasing plastic strain, i.e., the metal strain-hardens.
- The volume of the specimen remains constant during plastic deformation, AL = $A_0L_0$, and as the specimen elongates, it decreases uniformly along the gage length in crosssectional area.
- Initially the strain hardening more than compensates for this decrease in area and the engineering stress (proportional to load P) continues to rise with increasing strain.
- Eventually a point is reached where the decrease in specimen cross-sectional area is greater than the increase in deformation load arising from strain hardening.

- This condition will be reached first at some point in the specimen that is slightly weaker than the rest.
- All further plastic deformation is concentrated in this region, and the specimen begins to neck or thin down locally.
- Because the cross-sectional area now is decreasing far more rapidly than the deformation load is increased by strain hardening, the actual load required to deform the specimen falls off and the engineering stress by Eq. (8-1) likewise continues to decrease until fracture occurs.

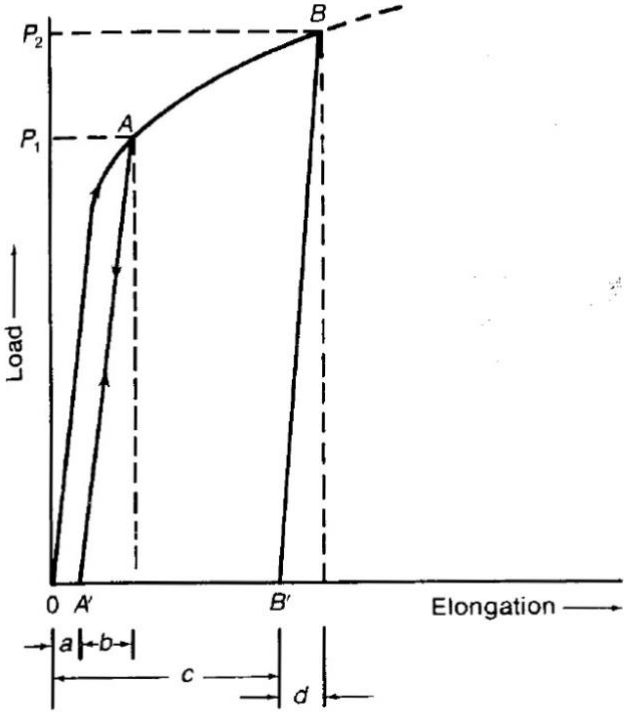


Figure 8-2 Loading and unloading curves showing elastic recoverable strain and plastic deformation.

- Consider a tensile specimen that has been loaded to a value in excess of the yield stress and then the load is removed (Fig. 8-2).
- The loading follows the path O-A-A'. Note that the slope of the unloading curve A-A' is parallel to the elastic modulus on loading.

- The recoverable elastic strain on unloading is $b = {}^{\sigma}/_{E} = ({}^{P1}/_{A_0})/E$.

- The permanent plastic deformation is the offset "a" in Fig. 8-2. Note that elastic deformation is always present in the tension specimen when it is under load.
- If the specimen were loaded and unloaded along the path 0-A-B-B' the elastic strain would be greater than on loading to $P_1$, since $P_2 > P_1$ but the elastic deformation (d) would be less than the plastic deformation (c).

**Tensile Strength**

- The tensile strength, or ultimate tensile strength (UTS), is the maximum load divided by the original cross-sectional area of the specimen.

$$S_u = \frac{P_{max}}{A_0} \qquad (8.3)$$

- The tensile strength is the value most often quoted from the results of a tension test; yet in reality it is a value of little fundamental significance with regard to the strength of a metal.
- For ductile metals the tensile strength should be regarded as a measure of the maximum load which a metal can withstand under the very restrictive conditions of uniaxial loading.
- It will be shown that this value bears little relation to the useful strength of the metal under the more complex conditions of stress which are usually encountered. For many years it was customary to base the strength of members on the tensile strength, suitably reduced by a factor of safety.
- The current trend is to the more rational approach of basing the static design of ductile metals on the yield strength. However, because of the long practice of using the tensile strength to determine the strength of materials, it has become a very familiar property, and as such it is a very useful identification of a material in the same sense that the chemical composition serves to identify a metal or alloy.
- Extensive empirical correlations between tensile strength and properties such as hardness and fatigue strength are often quite useful. For brittle materials, the tensile strength is a valid criterion for design. **Measures of Yielding**
- The stress at which plastic deformation or yielding is observed to begin depends on the sensitivity of the strain measurements.

• With most materials there is a gradual transition from elastic to plastic behavior, and the point at which plastic deformation begins is hard to define with precision.

• Various criteria for the initiation of yielding are used depending on the sensitivity of the strain measurements and the intended use of the data.

(1) True elastic limit based on micro strain measurements at strains on order of 2 x 10 6 (see Sec. 4-13). This elastic limit is a very low value and is related to the motion of a few hundred dislocations.

(2) Proportional limit is the highest stress at which stress is directly proportional to strain. It is obtained by observing the deviation from the straight-line portion of the stress-strain curve.

(3) Elastic limit is the greatest stress the material can withstand without any measurable permanent strain remaining on the complete release of load. With increasing sensitivity of strain measurement, the value of the elastic limit is decreased until at the limit it equals the true elastic limit determined from micro strain measurements. With the sensitivity of strain usually employed in engineering studies ($10^{-4}$), the elastic limit is greater than the proportional limit. Determination of the elastic limit requires a tedious incremental loading unloading test procedure.

(4) The yield strength is the stress required to produce a small specified amount of plastic deformation. The usual definition of this property is the offset yield strength determined by the stress corresponding to the intersection of the stress-strain curve and a line parallel to the elastic part of the curve offset by a specified strain (Fig. 81). In the United States the offset is usually specified as a strain of 0.2 or 0.1 percent (e = 0.002 or 0.001).

$$s_0 = \frac{P_{(\text{strain offset} = 0.002)}}{A_0} \qquad (8.4)$$

• A good way of looking at offset yield strength is that after a specimen has been loaded to its 0.2 percent offset yield strength and then unloaded it will be 0.2 percent longer than before the test.

• The offset yield strength is often referred to in Great Britain as the proof stress, where offset values are either 0.1 or 0.5 percent.

- The yield strength obtained by an offset method is commonly used for design and specification purposes because it avoids the practical difficulties of measuring the elastic limit or proportional limit.
- Some materials have essentially no linear portion to their stress-strain curve, for example, soft copper or gray cast iron. For these materials the offset method cannot be used and the usual practice is to define the yield strength as the stress to produce some total strain, for example, e = 0.005.

**Measures of Ductility**

- At our present degree of understanding, ductility is a qualitative, subjective property of a material. In general, measurements of ductility are of interest in three ways:

(1) To indicate the extent to which a metal can be deformed without fracture in metalworking operations such as rolling and extrusion.

(2) To indicate to the designer, in a general way, the ability of the metal to flow plastically before fracture. A high ductility indicates that the material is "forgiving" and likely to deform locally without fracture should the designer err in the stress calculation or the prediction of severe loads.

(3) To serve as an indicator of changes in impurity level or processing conditions. Ductility measurements may be specified to assess material "quality" even though no direct relationship exists between the ductility measurement and performance in service.

- The conventional measures of ductility that are obtained from the tension test are the engineering strain at fracture $e_f$ (usually called the elongation) and the reduction of area at fracture q. Both of these properties are obtained after fracture by putting the specimen back together and taking measurements of $L_f$ and $A_f$.

$$e_f = \frac{L_f - L_0}{L_0} \tag{8.5}$$

$$q = \frac{A_0 - A_f}{A_0} \tag{8.6}$$

- Both elongation and reduction of area usually are expressed as a percentage.
- Because an appreciable fraction of the plastic deformation will be concentrated in the necked region of the tension specimen, the value of will depend on the gage length $L_0$ over which the measurement was taken (see Sec. 8-5).
- The smaller the gage length the greater will be the contribution to the overall elongation from the necked region and the higher will be the value of ef.
- Therefore, when reporting values of percentage elongation, the gage length $L_0$ always should be given.
- The reduction of area does not suffer from this difficulty. Reduction of area values can be converted into an equivalent zero-gage-length elongation $e_0$.
- From the constancy of volume relationship for plastic deformation $AL = A_0L_0$, we obtain

$$\frac{L}{L_0} = \frac{A_0}{A} = \frac{1}{1-q}$$

$$e_0 = \frac{L - L_0}{L_0} = \frac{A_0}{A} - 1 = \frac{1}{1-q} - 1 = \frac{q}{1-q} \qquad (8\text{-}7)$$

- This represents the elongation based on a very short gage length near the fracture.

**Modulus of Elasticity**

- The slope of the initial linear portion of the stress-strain curve is the modulus of elasticity, or Young's modulus.
- The modulus of elasticity is a measure of the stiffness of the material.
- The greater the modulus, the smaller the elastic strain resulting from the application of a given stress.
- Since the modulus of elasticity is needed for computing deflections of beams and other members, it is an important design value.
- The modulus of elasticity is determined by the binding forces between atoms.
- Since these forces cannot be changed without changing the basic nature of the material, it follows that the modulus of elasticity is one of the most structure-insensitive of the mechanical properties.
- It is only slightly affected by alloying additions, heat treatment, or cold-work.

- However, increasing the temperature decreases the modulus of elasticity. The modulus is usually measured at elevated temperatures by a dynamic method.
- Typical values3 of the modulus of elasticity for common engineering metals at different temperatures are given in Table 8-1. **Resilience**
- The ability of a material to absorb energy when deformed elastically and to return it when unloaded is called resilience.
- This is usually measured by the modulus of resilience, which is the strain energy per unit volume required to stress the material from zero stress to the yield stress $\sigma_0$.
- Referring to Eq. (2-80), the strain energy per unit volume for uniaxial tension is

$$U_0 = \tfrac{1}{2}\sigma_x e_x$$

- From the above definition the modulus of resilience is

$$U_R = \frac{1}{2} s_0 e_0 = \frac{1}{2} s_0 \frac{s_0}{E} = \frac{s_0^2}{2E} \qquad (8.8)$$

- This equation indicates that the ideal material for resisting energy loads in applications where the material must not undergo permanent distortion, such as mechanical springs, is one having a high yield stress and a low modulus of elasticity.

**Toughness**

- The toughness of a material is its ability to absorb energy in the plastic range. The ability to withstand occasional stresses above the yield stress without fracturing is particularly desirable in parts such as freight-car couplings, gears, chains, and crane hooks.
- Toughness is a commonly used concept which is difficult to pin down and define. One way of looking at toughness is to consider that it is the total area under the stress-strain curve.

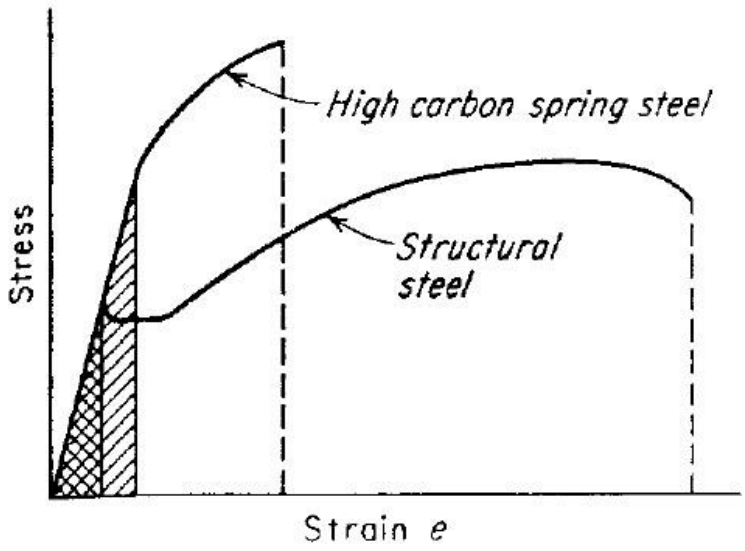


Figure 8-3 Comparison of stress-strain curves for high Strain e and low-toughness materials.

- This area is an indication of the amount of work per unit volume which can be done on the material without causing it to rupture.
- Figure 8-3 shows the stress-strain curves for high- and low-toughness materials.
- The high-carbon spring steel has a higher yield strength and tensile strength than the medium-carbon structural steel.
- However, the structural steel is more ductile and has a greater total elongation. The total area under the stress-strain curve is greater for the structural steel, and therefore it is a tougher material.
- This illustrates that toughness is a parameter which comprises both strength and ductility.
- The crosshatched regions in Fig. 8-3 indicate the modulus of resilience for each steel.

Because of its higher yield strength, the spring steel has the greater resilience.

- Several mathematical approximations for the area under the stress-strain curve have been suggested.
- For ductile metals which have a stress-strain curve like that of the structural steel, the area under the curve can be approximated by either of the following equations:

$$U_T \approx s_u e_f$$

$$U_T \approx \frac{s_0 + s_u}{2} e_f \qquad (8.9 \& 8.10)$$

- For brittle materials the stress-strain curve is sometimes assumed to be a parabola, and the area under the curve is given by

$$U_T \approx \frac{2}{3} s_u e_f \tag{8.11}$$

- All these relations are only approximations to the area under the stress-strain curves.

## 8-2 TRUE-STRESS-TRUE-STRAIN CURVE

- The engineering stress-strain curve does not give a true indication of the deformation
- characteristics of a metal because it is based entirely on the original dimensions of the specimen, and these dimensions change continuously during the test.
- Also, ductile metal which is pulled in tension becomes unstable and necks down during the course of the test. Because the cross-sectional area of the specimen is decreasing rapidly at this stage in the test, the load required to continue deformation falls off.
- The average stress based on original area likewise decreases, and this produces the falloff in the stress-strain curve beyond the point of maximum load.
- Actually, the metal continues to strain-harden all the way up to fracture, so that the stress required to produce further deformation should also increase.
- If the true stress, based on the actual cross-sectional area of the specimen, is used, it is found that the stress-strain curve increases continuously up to fracture.
- If the strain measurement is also based on instantaneous measurements, the curve which is obtained is known as a true-stress-true-strain curve.
- This is also known as a flow curve (Sec. 3-2) since it represents the basic plastic-flow characteristics of the material.
- Any point on the flow curve can be considered the yield stress for a metal strained in tension by the amount shown on the curve.
- Thus, if the load is removed at this point and then reapplied, the material will behave elastically throughout the entire range of reloading.
- The true stress **σ** is expressed in terms of engineering stress **s** by

$$\sigma = \frac{P}{A_0}(e + 1) = s(e + 1) \tag{8.12}$$

- The derivation of Eq. (8-12) assumes both constancy of volume and a homogeneous distribution of strain along the gage length of the tension specimen.
- Thus, Eq. (8-12) should only be used until the onset of necking.
- Beyond maximum load the true stress should be determined from actual measurements of load and cross-sectional area.

$$\sigma = P/A \tag{8.13}$$

- The true strain e may be determined from the engineering or conventional strain e by

$$\varepsilon = \ln(e + 1) \tag{8.14}$$

- This equation is applicable only to the onset of necking for the reasons discussed above. Beyond maximum load the true strain should be based on actual area or diameter measurements.

$$\varepsilon = \ln \frac{A_0}{A} = \ln \frac{(\pi/4) D_0^2}{(\pi/4) D^2} = 2 \ln \frac{D_0}{D} \tag{8.15}$$

- Figure 8-4 compares the true-stress-true-strain curve with its corresponding engineering stress-strain curve.
- Note that because of the relatively large plastic strains, the elastic region has been compressed into the y axis.
- In agreement with Eqs. (8-12) and (8-14), the true-stress-true-strain curve is always to the left of the engineering curve until the maximum load is reached.
- However, beyond maximum load the high localized strains in the necked region that are used in Eq. (8-15) far exceed the engineering strain calculated from Eq. (8-2).
- Frequently the flow curve is linear from maximum load to fracture, while in other cases its slope continuously decreases up to fracture.
- The formation of a necked region or mild notch introduces triaxial stresses which make it difficult to determine accurately the longitudinal tensile stress on out to fracture. **True Stress at Maximum Load**

- The true stress at maximum load corresponds to the true tensile strength.
- For most materials necking begins at maximum load at a value of strain where the true stress equals the slope of the flow curve (see Sec. 8-3).
- Let $\sigma_u$ and $e_u$ denote the true stress and true strain at maximum load when the crosssectional area of the specimen is Au.
- The ultimate tensile strength is given by

$$\sigma_u = s_u \frac{A_0}{A_u}$$

$$\sigma_u = s_u e^{\epsilon_u}$$

$$s_u = \frac{P_{\max}}{A_0}$$

$$\sigma_u = \frac{P_{\max}}{A_u} \qquad \epsilon_u = \ln \frac{A_0}{A_u}$$

Eliminating $P_{max}$ yields

(8.16)

**True Fracture Stress**

- The true fracture stress is the load at fracture divided by the cross-sectional area at fracture.

- This stress should be corrected for the triaxial state of stress existing in the tensile specimen at fracture. Since the data required for this correction are often not available, true-fracture-stress values are frequently in error.

**True Fracture Strain**

- The true fracture strain $e_f$ is the true strain based on the original area A0 and the area after fracture $A_f$.

$$\varepsilon_f = \ln \frac{A_0}{A_f} \qquad (7.17)$$

- This parameter represents the maximum true strain that the material can withstand before fracture and is analogous to the total strain to fracture of the engineering stressstrain curve.
- Since Eq. (8-14) is not valid beyond the onset of necking, it is not possible to calculate $e_f$ from measured values of However, for cylindrical tensile specimens the reduction of area q is related to the true fracture strain by the relationship

$$\varepsilon_f = \ln \frac{1}{1 - q} \qquad (8.18)$$

**True Uniform Strain**

- The true uniform strain £w is the true strain based only on the strain up to maximum load.
- It may be calculated from either the specimen cross-sectional area $A_{max}$ the gage length $L_u$ at maximum load.
- Equation (8-14) may be used to convert conventional uniform strain to true uniform strain. The uniform strain is often useful in estimating the formability of metals from the results of a tension test.

$$\varepsilon_u = \ln \frac{A_0}{A_u} \quad (8.19)$$

**True Local Necking Strain**

- The local necking strain $\varepsilon_n$ is the strain required to deform the specimen from maximum load to fracture.

$$\varepsilon_n = \ln \frac{A_u}{A_f} \quad (8.20)$$

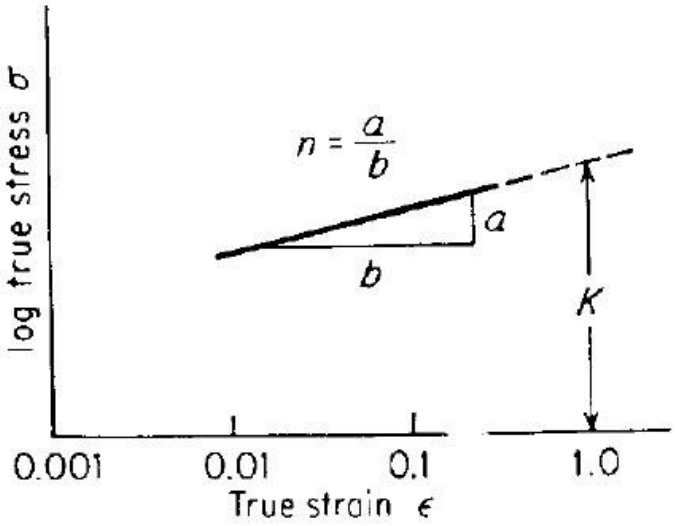


Figure 8-5 Log-log plot of true stress-strain curve.

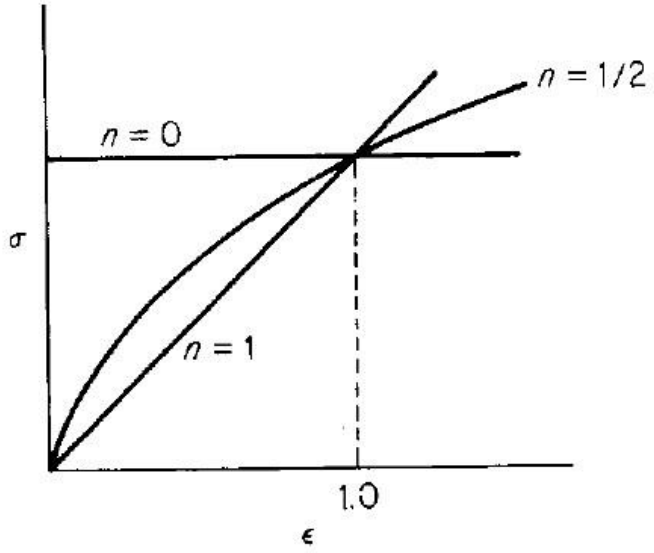


Figure 8-6 Various forms of power curve $\sigma = k\varepsilon^n$

**Table 8-3 Values for *n* and *K* for metals at room temperature**

| Metal | Condition | *n* | *K*, MPa | Ref. |
|---|---|---|---|---|
| 0.05% C steel | Annealed | 0.26 | 530 | † |
| SAE 4340 steel | Annealed | 0.15 | 640 | † |
| 0.6% C steel | Quenched and tempered 540°C | 0.10 | 1570 | ‡ |
| 0.6% C steel | Quenched and tempered 705°C | 0.19 | 1230 | ‡ |
| Copper | Annealed | 0.54 | 320 | † |
| 70/30 brass | Annealed | 0.49 | 900 | ‡ |

- The low curve of many metals in the region of uniform plastic deformation can be expressed by the simple power curve relation

$$\sigma = K\varepsilon^n \tag{8.21}$$

- Where n is the strain-hardening exponent and K is the strength coefficient.  A log-log plot of true stress and true strain up to maximum load will result in a  Straight line if Eq. (8-21) is satisfied by the data (Fig. 8-5).
- The linear slope of this line is n and K is the true stress at e - 1.0 (corresponds to q = 0.63).
- The strain-hardening exponent1 may have values from n - 0 (perfectly plastic solid) to n - 1 (elastic solid) (see Fig. 8-6).
- For most metals n has values between 0.10 and 0.50 (see Table 8-3).
- It is important to note that the rate of strain hardening dσ/dε is not identical with the strain-hardening exponent.

From the definition of n

$$n = \frac{d(\log \sigma)}{d(\log \varepsilon)} = \frac{d(\ln \sigma)}{d(\ln \varepsilon)} = \frac{\varepsilon}{\sigma}\frac{d\sigma}{d\varepsilon}$$

$$\frac{d\sigma}{d\varepsilon} = n\frac{\sigma}{\varepsilon} \tag{8.22}$$

- There is nothing basic about Eq. (8-21) and deviations from this relationship frequently are observed, often at low strains ($10^{-3}$) or high strains (ε == 1.0). One common type of deviation is for a log-log plot of Eq. (8-21) to result in two straight

lines with different slopes. Sometimes data which do not plot according to Eq. (8-21) will yield a straight line according to the relationship

$$\sigma = K(\varepsilon_0 + \varepsilon)^n \tag{8.23}$$

Datsko has shown how e0 can be considered to be the amount of strain hardening that the material received prior*to the tension test.

- Another common variation in Eq. (8-21) is the Ludwik equation
- $$\sigma = \sigma_0 + K\varepsilon^n \tag{8.24}$$
- where $\sigma_0$ is the yield stress and K and n are the same constants as in Eq. (8-21).
- This equation may be more satisfying than Eq. (8-21) since the latter implies that at zero true strain the stress is zero.
- Morrison1 has shown that σ0 can be obtained from the intercept of the strain-hardening portion of the stress-strain curve and the elastic modulus line by

$$\sigma_0 = \left(\frac{K}{E^n}\right)^{1/1-n}$$

- The true-stress-true-strain curve of metals such as austenitic stainless steel, which deviate markedly from Eq. (8-21) at low strains, can be expressed by

$$\sigma = K\varepsilon^n + e^{K_1}e^{n_1\varepsilon}$$

- where $e^{K1}$ is approximately equal to the proportional limit and $n_l$ is the slope of the deviation of stress from Eq. (8-21) plotted against ε. Still other expressions for the flow curve have been discussed in the literature.

## 8-3 INSTABILITY IN TENSION

- Necking generally begins at maximum load during the tensile deformation of a ductile metal. An ideal plastic material in which no strain hardening occurs would become unstable in tension and begin to neck just as soon as yielding took place.
- However, a real metal undergoes strain hardening, which tends to increase the loadcarrying capacity of the specimen as deformation increases.
- This effect is opposed by the gradual decrease in the cross-sectional area of the specimen as it elongates.

- Necking or localized deformation begins at maximum load, where the increase in stress due to decrease in the cross-sectional area of the specimen becomes greater than the increase in the load-carrying ability of the metal due to strain hardening.
- This condition of instability leading to localized deformation is defined by the condition dP = 0.

$$P = \sigma A$$
$$dP = \sigma\, dA + A\, d\sigma = 0$$

From the constancy-of-volume relationship,

$$\frac{dL}{L} = -\frac{dA}{A} = d\varepsilon$$

and from the instability condition

$$-\frac{dA}{A} = \frac{d\sigma}{\sigma}$$

so that at a point of tensile instability

$$\frac{d\sigma}{d\varepsilon} = \sigma \qquad (8.25)$$

- Therefore, the point of necking at maximum load can be obtained from the true-stresstrue-strain curve1 by finding the point on the curve having a subtangent of unity (Fig.

8-la) or the point where the rate of strain hardening equals the stress (Fig. 8-76)

The necking criterion can be expressed more explicitly if engineering strain is used. Starting with Eq. (8-25),

$$\frac{d\sigma}{d\varepsilon} = \frac{d\sigma}{de}\frac{de}{d\varepsilon} = \frac{d\sigma}{de}\frac{dL/L_0}{dL/L} = \frac{d\sigma}{de}\frac{L}{L_0} = \frac{d\sigma}{de}(1+e) = \sigma$$

$$\frac{d\sigma}{de} = \frac{\sigma}{1+e} \qquad (8.26)$$

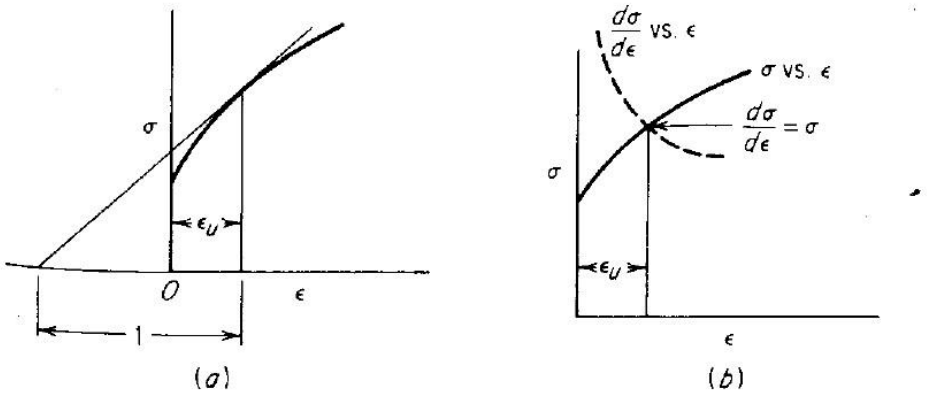


**Figure 8-7** Graphical interpretation of necking criterion.

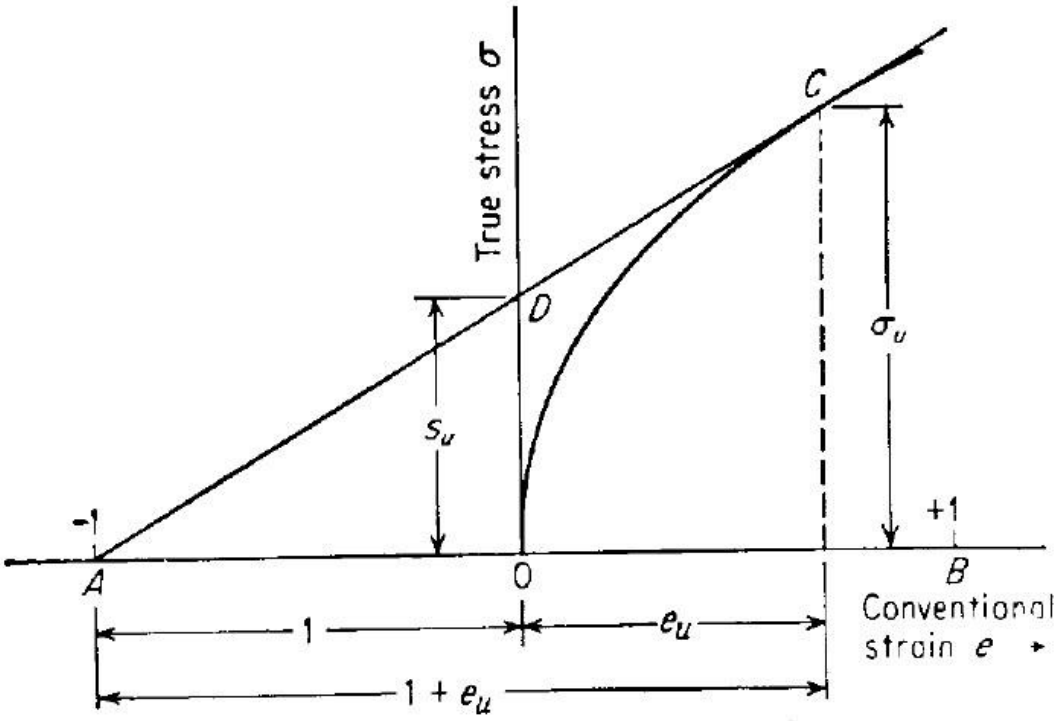


Figure 8-8 Considere's construction for the determination of the point of maximum load.

- Equation (8-26) permits an interesting geometrical construction called Considered construction for the determination of the point of maximum load.
- In Fig. 8-8 the stress-strain curve is plotted in terms of true stress against conventional linear strain.

- Let point A represent a negative strain of 1.0. A line drawn from point A which is tangent to the stress-strain curve will establish the point of maximum load, for according to Eq. (8-26) the slope at this point is $\sigma/(1+e)$
- By substituting the necking criterion given in Eq. (8-25) into Eq. (8-22), we obtain a simple relationship for the strain at which necking occurs. This strain is the true uniform strain $\varepsilon_u$.

$$\frac{d\sigma}{d\varepsilon} = \sigma$$

$$\frac{d\sigma}{d\varepsilon} = n\frac{\sigma}{\varepsilon}$$

$$\varepsilon_u = n \qquad (8.27)$$

Necking in a cylindrical tensile specimen is symmetrical around the tensile axis if the material is isotropic.

- However, a different type of necking behavior is found for a tensile specimen with rectangular cross section that is cut from a sheet.
- For a sheet tensile specimen where width is much greater than thickness there are two types of tensile flow instability.
- The first is diffuse necking, so called because its extent is much greater than the sheet thickness (Fig. 8-9).
- This form of unstable flow in a sheet tensile specimen is analogous to the neck formed in a cylindrical tensile specimen.
- Diffuse necking initiates according to the relationships discussed above.
- Diffuse necking may terminate in fracture but it often is followed by a second instability process called localized necking.
- In this mode the neck is a narrow band with a width about equal to the sheet thickness inclined at an angle to the specimen axis, across the width of the specimen (Fig. 8-9).

- In localized necking there is no change in width measured along the trough of the localized neck, so that localized necking corresponds to a state of plane-strain deformation.

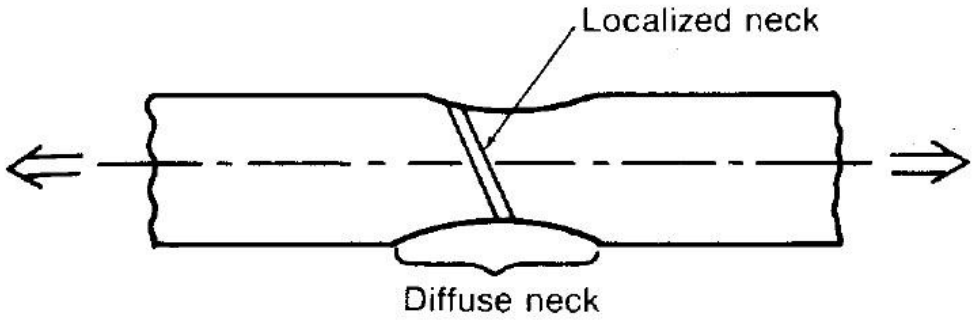


Figure 8-9 Illustration of diffuse necking and localized necking in a sheet tensile specimen.

- With localized necking the decrease in specimen area with increasing strain (the geometrical softening) is restricted to the thickness direction.
- Thus, dA = wdt where w is the constant length of the localized neck and t is the thickness of the neck.

$$\frac{dP}{d\varepsilon}\left(\frac{1}{A}\right) = -\frac{\sigma w\, dt}{d\varepsilon}\left(\frac{1}{A}\right) = -\frac{\sigma w\, dt}{wt\, d\varepsilon} = -\sigma\frac{dt/t}{d\varepsilon} \qquad (8\text{-}28)$$

- Let the direction of axial strain be $\varepsilon_1$, the width strain be $\varepsilon_2$, and the thickness strain be $\varepsilon_3$.

- From constancy of volume, $d\varepsilon_2 + d\varepsilon_3 = {}^{-d\varepsilon_1}/_2$
- Substituting into Eq. (8-28) gives $d\varepsilon_1/2$, and $d\varepsilon_3 = dt/t$

$$\frac{dP}{d\varepsilon}\left(\frac{1}{A}\right) = \frac{\sigma}{2} \qquad (8.29)$$

The increase in load-carrying ability due to strain hardening is given by

$$\frac{dP}{d\varepsilon}\left(\frac{1}{A}\right) = \frac{A\,d\sigma}{d\varepsilon}\left(\frac{1}{A}\right) = \frac{d\sigma}{d\varepsilon} \qquad (8.30)$$

- As before, necking begins when the geometrical softening just balances the strain hardening, so equating Eq. (8-29) and (8-30) gives

$$\frac{d\sigma}{d\varepsilon} = \frac{\sigma}{2} \qquad (8.31)$$

- This criterion for localized necking expresses the fact that the specimen area decreases with straining less rapidly in this mode than in diffuse necking.
- Thus, more strain must be accumulated before the geometrical softening will cancel the strain hardening.
- For a power-law low curve**, $\varepsilon_u = 2n$** for localized necking.

## 8-5 DUCTILITY MEASUREMENT IN TENSION TEST

- Having discussed in Sec. 8-1 the standard measurements of ductility that are obtained from the tension test, i.e., percent elongation and reduction of area, we return again to this subject armed with an understanding of the phenomenon of necking.
- The measured elongation from a tension specimen depends on the gage length of the specimen or the dimensions of its cross section.
- This is because the total extension consists of two components, the uniform extension up to necking and the localized extension once necking begins.
- The extent of uniform extension will depend on the metallurgical condition of the material (through n) and the effect of specimen size and shape on the development of the neck.
- Figure 8-11 illustrates the variation of the local elongation, Eq. (8-7), along the gage length of a prominently necked tensile specimen.
- It readily can be seen that the shorter the gage length the greater the influence of localized deformation at the neck on the total elongation of the gage length.

The extension of a specimen at fracture can be expressed by

$$L_f - L_0 = \alpha + e_u L_0 \tag{8.33}$$

Where a is the local necking extension and euL0 is the uniform extension. The tensile elongation then is given by

$$e_f = \frac{L_f - L_0}{L_0} = \frac{\alpha}{L_0} + e_u \tag{8.34}$$

- Which clearly indicates that the total elongation is a function of the specimen gage length. The shorter the gage length the greater the percentage elongation.
- Numerous attempts, dating back to about 1850, have been made to rationalize the strain distribution in the tension test.
- Perhaps the most general conclusion that can be drawn is that geometrically similar specimens develop geometrically similar necked regions.
- According to Barba's law, $\alpha = \beta\sqrt{A_0}$ , and the elongation equation becomes

$$e_f = \beta\frac{\sqrt{A_0}}{L_0} + e_u \tag{8.35}$$

**8-6 EFFECT OF STRAIN RATE ON FLOW PROPERTIES**

- The rate at which strain is applied to a specimen can have an important influence on the low stress.
- Strain rate is defined as $\dot{\varepsilon} = {}^{d\varepsilon}/_{dt}$, and is conventionally expressed in units of $s^{-1}$, i.e.,

"per second."

- The spectrum of available strain rates is given in Table 8-5.
- Figure 8-12 shows that increasing strain rate increases low stress. Moreover, the strainrate dependence of strength increases with increasing temperature.
- The yield stress and low stress at lower plastic strains are more dependent on strain rate than the tensile strength.

- High rates of strain cause the yield point to appear in tests on low-carbon steel that do not show a yield point under ordinary rates of loading.

**Table 8-5 Spectrum of strain rate**

| Range of strain rate | Condition or type test |
|---|---|
| $10^{-8}$ to $10^{-5}$ $s^{-1}$ | Creep tests at constant load or stress |
| $10^{-5}$ to $10^{-1}$ $s^{-1}$ | "Static" tension tests with hydraulic or screw-driven machines |
| $10^{-1}$ to $10^{2}$ $s^{-1}$ | Dynamic tension or compression tests |
| $10^{2}$ to $10^{4}$ $s^{-1}$ | High-speed testing using impact bars (must consider wave propagation effects) |
| $10^{4}$ to $10^{8}$ $s^{-1}$ | Hypervelocity impact using gas guns or explosively driven projectiles (shock-wave propagation) |

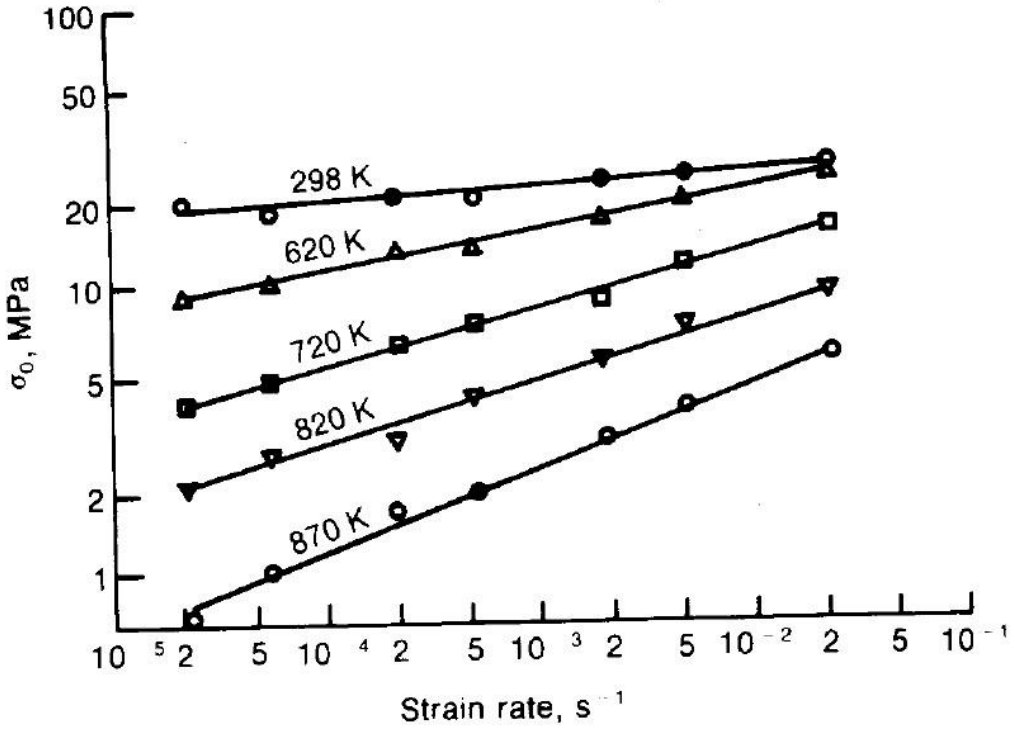


Figure 8-12 Flow stress at a = 0.002 versus strain rate for 6063-0 aluminum alloy

- Nadai has presented a mathematical analysis of the conditions existing during the extension of cylindrical specimen with one end fixed and the other attached to the movable crosshead of the testing machine.
- The crosshead velocity is v = dL/dt,
- The strain rate expressed in terms of conventional linear strain is $\dot{e}$.

$$\dot{e} = \frac{de}{dt} = \frac{d(L - L_0)/L_0}{dt} = \frac{1}{L_0}\frac{dL}{dt} = \frac{v}{L_0} \tag{8.36}$$

- Thus, the conventional strain rate is proportional to the crosshead velocity. In a modern testing machine in which the crosshead velocity can be set accurately and controlled, it is a simple matter to carry out tension tests at constant conventional strain rate.

The true strain rate e is given by

$$\dot{\varepsilon} = \frac{d\varepsilon}{dt} = \frac{d\left[\ln\left(L/L_0\right)\right]}{dt} = \frac{1}{L}\frac{dL}{dt} = \frac{v}{L} \tag{8.37}$$

The true strain rate is related to the conventional strain rate by the following equation:

$$\dot{\varepsilon} = \frac{v}{L} = \frac{L_0}{L}\frac{de}{dt} = \frac{1}{1+e}\frac{de}{dt} = \frac{\dot{e}}{1+e} \tag{8.38}$$

**Close Loop Control:**

- Equation (8-37) indicates that for a constant crosshead speed the true-strain rate will decrease as the specimen elongates.
- To maintain a constant true-strain rate using open-loop control the deformation velocity must increase in proportion to the increase in the length of the specimen1 or must increase as

$$v = \dot{\varepsilon} L_0 \exp\left(\dot{\varepsilon} t\right) \tag{8.39}$$

**Open Loop Control:**

- When plastic flow becomes localized or non-uniform along the gage length then openloop control no longer is satisfactory.
- Now it is necessary to monitor the instantaneous cross section of the deforming region using closed-loop control

- For deformation occurring at constant volume a constant true-strain rate is obtained if the specimen area changes as

$$A = A_0 \exp(-\dot{\varepsilon} t) \qquad (8.40)$$

As Fig. 8-12 indicates, a general relationship between low stress and strain rate, at constant strain and temperature is

$$\sigma = C(\dot{\varepsilon})^m|_{\varepsilon, T}$$

- where m is known as the strain-rate sensitivity.
- The exponent m can be obtained from the slope of a plot of log σ vs. log $\dot{\varepsilon}$, like Fig. 8-12.
- However, a more sensitive way is a rate-change test in which m is determined by measuring the change in flow stress brought about by a change in $\dot{\varepsilon}$ at a constant $\dot{\varepsilon}$ and T (see Fig. 8-13).

$$m = \left(\frac{\partial \ln \sigma}{\partial \ln \dot{\varepsilon}}\right)_{\varepsilon, T} = \frac{\dot{\varepsilon}}{\sigma}\left(\frac{\partial \sigma}{\partial \dot{\varepsilon}}\right)_{\varepsilon, T} = \frac{\Delta \log \sigma}{\Delta \log \dot{\varepsilon}} = \frac{\log \sigma_2 - \log \sigma_1}{\log \dot{\varepsilon}_2 \cdot \log \dot{\varepsilon}_1} = \frac{\log(\sigma_2/\sigma_1)}{\log(\dot{\varepsilon}_2/\dot{\varepsilon}_1)} \qquad (8.42)$$

- Strain-rate sensitivity of metals is quite low (< 0.1) at room temperature but m increases with temperature, especially at temperatures above half of the absolute melting point. In hot-working conditions m values of 0.1 to 0,2 are common.
- Equation (8-41) is not the best description of the strain-rate dependence of flow stress for steels. For these materials a semi logarithmic relationship between flow stress and strain rate appears to hold.

$$\sigma = k_1 + k_2 \ln \frac{\dot{\varepsilon}}{\varepsilon_0} \qquad (8.43)$$

where $k_1$ and $k_2$, and $\varepsilon_0$ are constants

**Superplasticity:**

- High strain-rate sensitivity is a characteristic of superplastic metals and alloys. Superplasticity refers to extreme extensibility with elongations usually between 100 and 1,000 percent.

- Superplastic metals have a grain size or interphase spacing of the order of 1 μm.
- Testing at high temperature and low strain rates accentuates superplastic behavior.
- While the mechanism of superplastic deformation is not yet well established, it is clear that the large elongations result from the suppression of necking in these materials with high values of m.
- An extreme case is hot glass (m = 1) which can be drawn from the melt into glass fibers without the fibers necking down.

## 8-7 EFFECT OF TEMPERATURE ON FLOW PROPERTIES

- The stress-strain curve and the low and fracture properties derived from the tension test are strongly dependent on the temperature at which the test was conducted.
- In general, strength decreases and ductility increases as the test temperature is increased. However, structural changes such as precipitation, strain aging, or recrystallization may occur in certain temperature ranges to alter this general behavior.
- Thermally activated processes assist deformation and reduce strength at elevated temperatures.
- At high temperatures and/or long exposure, structural changes occur resulting in timedependent deformation or creep.

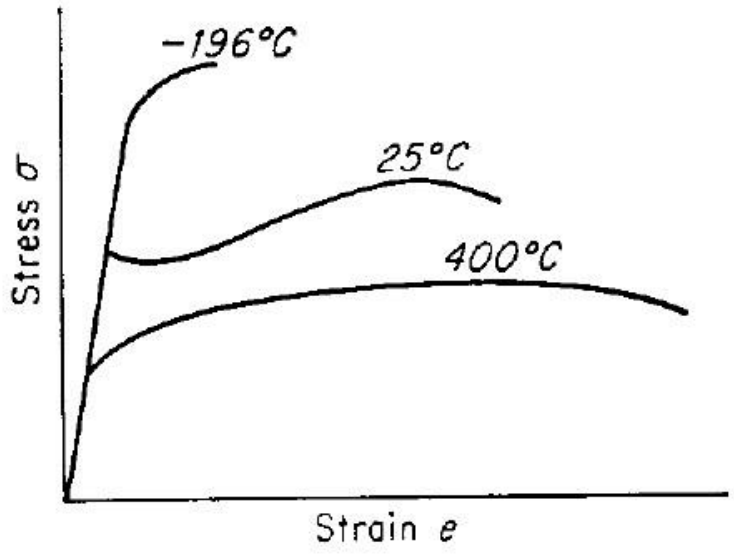


Figure 8-16 Changes in engineering stress-strain curves of mild steel with temperature.

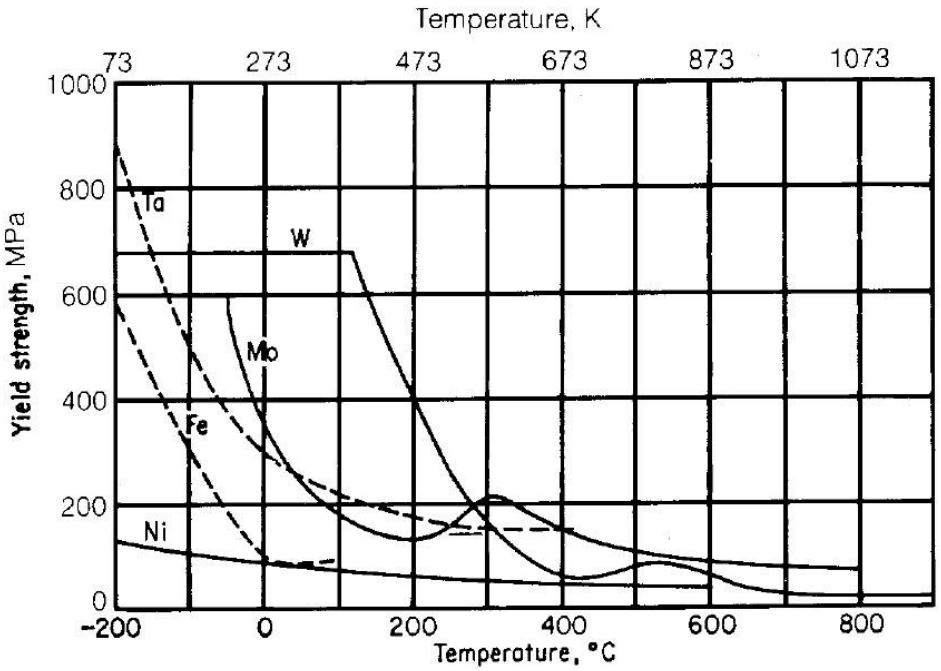


Figure 8-17 Effect of temperature on the yield strength of body-cantered cubic Ta, W, Mo, Fe, and face-cantered cubic Ni.

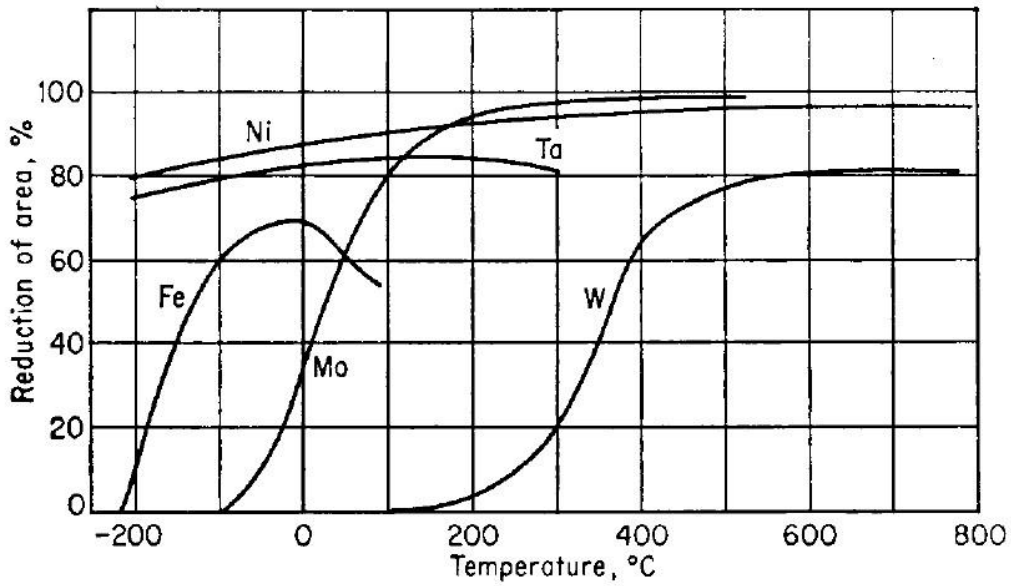


Figure 8-18 Effect of temperature on the reduction of area of Ta, W, Mo, Fe, and Ni.

- The change with temperature of the engineering stress-strain curve in mild steel is shown schematically in Fig. 8-16.
- Figure 8-17 shows the variation of yield strength with temperature for body-cantered cubic tantalum, tungsten, molybdenum, and iron and for face-cantered cubic nickel.

- Note that for the bcc metals the yield stress increases rapidly with decreasing temperature, while for nickel (and other fee metals) the yield stress is only slightly temperature-dependent.
- Based on the concept of fracture stress introduced in Sec. 7-11, and especially Fig. 717, it is easy to see why bcc metals exhibit brittle fracture at low temperatures.
- Figure 8-18 shows the variation of reduction of area with temperature for these same metals.
- Note that tungsten is brittle at 100 $^0$C (= 373 K), iron at – 225 $^0$C (= 48 K), while nickel decreases little in ductility over the entire temperature interval.
- In fcc metals flow stress is not strongly dependent on temperature but the strainhardening exponent decreases with increasing temperature.
- This results in the stress-strain curve flattening out with increasing temperature and the tensile strength being more temperature-dependent than the yield strength.
- Tensile deformation at elevated temperature may be complicated by the formation of more than one neck in the specimen.

**Homologous Temperature**

- The best way to compare the mechanical properties of different materials at various temperatures is in terms of the ratio of the test temperature to the melting point, expressed in degree kelvin.
- This ratio is often referred to as the homologous temperature. When comparing the low stress of two materials at an equivalent homologous temperature, it is advisable to correct for the effect of temperature on elastic modulus by comparing ratios of σ/E rather than simple ratios of flow stress.

The temperature dependence of flow stress at constant strain and strain rate generally can be represented by

$$\sigma = C_2 e^{Q/RT}\big|_{\varepsilon,\dot{\varepsilon}} \qquad (8.51)$$

where Q = an activation energy for plastic flow, J mol$^{-1}$

R = universal gas constant, 8.314 J mol $^{-1}$ K$^{-1}$

T = testing temperature, K

If this expression is obeyed, a plot of In σ versus 1/T will give a straight line with a slope Q/R.

## 8-8 INFLUENCE OF TESTING MACHINE ON FLOW PROPERTIES

- Two general types of machines are used in tension testing: (1) load controlled machines and (2) displacement controlled machines.
- In load controlled machines the operator adjusts the load precisely but must live with whatever displacement happens to be associated with the load.
- The older type hydraulic machines are of this type.
- In the displacement controlled machine the displacement is controlled and the load adjusts itself to that displacement.
- The popular screw-driven machines in which the crosshead moves to a predetermined constant velocity are of this type.
- The more recently developed servo hydraulic testing machines provide both load or displacement control.
- These versatile machines are well adapted to computer control.
- In a non - automated testing system the servo-control is limited to control of load, stroke, or strain.
- However, with modern computer control it is possible to conduct tests based on the control of calculated variables such as true strain or stress intensity factor.

**Total Strain:**

- All testing machines deflect under load.
- Therefore, we cannot directly convert the crosshead motion velocity into deformation of the specimen without appropriate corrections.
- A constant crosshead velocity testing machine applies a constant total strain rate that is the sum of
  (1) the elastic strain rate in the specimen,
  (2) the plastic strain rate in the specimen, and
  (3) the strain rate

Resulting from the elasticity of the testing machine.

- At any instant of time there is some distribution of strain rate between these components.
- If the cross- head velocity is v, then at a particular time t the total displacement is vt.
- The force P on the specimen causes an elastic machine displacement P/K.
- The elastic displacement of the specimen (from Hooke's law) is σL/E and the plastic displacement of the specimen is $\varepsilon_p L$.

Since the total displacement is the sum of its components

$$vt = \frac{P}{K} + \frac{\sigma L}{E} + \varepsilon_p L \qquad (8.55)$$

Solving for $\varepsilon_p$, we see that the plastic strain taken from a load-time chart on a constant crosshead-velocity testing machine must be corrected for machine stiffness as well as specimen elasticity.

$$\varepsilon_p = \frac{vt}{L} - \frac{\sigma}{E} - \frac{P}{KL} \qquad (8.56)$$

## FRACTURE

## 7-1 INTRODUCTION

- **Fracture** is the s**eparation, or fragmentation, of a solid body into two or more parts** under the action of stress.
- The process of fracture can be considered to be made up of **two components, crack initiation and crack propagation.**
- Fractures can be c**lassified into two general categories**, **ductile fracture and brittle fracture.**
- **A ductile fracture is characterized by appreciable plastic deformation prior to and during the propagation of the crack. An appreciable amount of gross deformation is usually present at the fracture surfaces.**
- **Brittle fracture in metals is characterized by a rapid rate of crack propagation, with no gross deformation and very little micro deformation. It is akin to cleavage in ionic crystals.**
- The **tendency for brittle fracture is increased with decreasing temperature, increasing strain rate, and triaxial stress conditions (usually produced by a notch).**
- **Brittle fracture is to be avoided at all cost, because it occurs without warning and usually produces disastrous consequences.**

## 7-2 TYPES OF FRACTURE IN METALS

- Metals can exhibit many different types of fracture, depending on the **material, temperature, state of stress, and rate of loading.**
- The two broad categories of **ductile and brittle fracture** have already been considered.
- Figure 7-1 schematically illustrates some of the types of tensile fractures which can occur in metals.
- A **brittle fracture** (Fig. 1-la) is characterized by separation normal to the tensile stress. Outwardly there is no evidence of deformation, although with x-ray diffraction analysis it is possible to detect a thin layer of deformed metal at the fracture surface.
- **Brittle fractures** have been observed in **bcc and hcp metals**, but not in **fcc metals unless there are factors contributing to grain-boundary embrittlement**.

**Ductile fractures** can take several forms. Single crystals of hcp metals **may slip on successive basal planes** until finally the crystal separates by shear (Fig.7-1b).

- **Polycrystalline specimens** of very ductile metals, like **gold or lead, may actually be drawn down to a point before they rupture** (Fig. 7- l c).
- In the tensile fracture of moderately ductile metals the plastic deformation eventually produces a necked region (Fig. 1- l d).

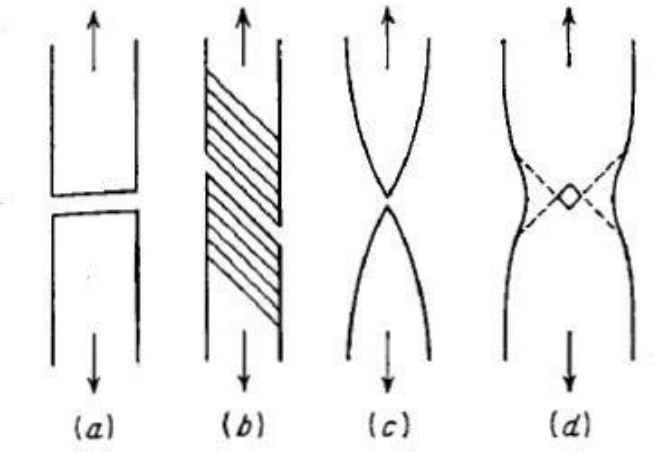


Figure 7-1 Types of fractures observed in metal subjected to uniaxial tension, (a) Brittle fracture of single crystals and polycrystals; (b) shearing fracture in ductile single crystals; (c) completely ductile fracture in polycrystals; (d) ductile fracture in polycrystals.

- Fracture begins at the center of the specimen and then extends by a shear separation along the dashed lines in Fig. 7- l d. This results in the familiar **"cup-and-cone"** fracture.
- **Fractures are classified** with respect to **several characteristics**, such as **strain to fracture, crystallographic mode of fracture, and the appearance of the fracture**.

**Gansamer has summarized the terms commonly used** to describe fractures as follows

| Behavior described | Terms used | |
|---|---|---|
| Crystallographic mode | Shear | Cleavage |
| Appearance of fracture | Fibrous | Granular |
| Strain to fracture | Ductile | Brittle |

A **shear fracture** occurs as the result of extensive slip on the active slip plane. This type of fracture is promoted by **shear stresses**.

- The **cleavage mode of fracture is controlled by tensile stresses** acting normal to a crystallographic cleavage plane.
- A **fracture surface which is caused by shear appears at low magnification to be gray and fibrous,** while a **cleavage fracture appears bright or granular, owing to reflection of light from the flat cleavage surfaces.**
- Fracture surfaces frequently consist of a **mixture of fibrous and granular fracture,** and it is customary to report the percentage of the surface area represented by one of these categories.
- Based on metallographic examination, fractures in **polycrystalline samples** are classified as either ***transgranular*** (***the crack propagates through the grains***) or ***intergranular*** (***the crack propagates along the grain boundaries***).
- A **ductile fracture is one which exhibits a considerable degree of deformation**. The boundary between a **ductile and brittle fracture is arbitrary** and depends on the situation being considered.
- For example, **nodular cast iron is ductile when compared with ordinary gray iron**; yet it would be considered **brittle when compared with mild steel**.
- As a further example, a deeply notched tensile specimen will exhibit little gross deformation; yet the fracture could occur by a shear mode.

## 7-3 THEORETICAL COHESIVE STRENGTH OF METALS

- Metals are of great technological value, primarily because of their **high strength combined with a certain measure of plasticity**.
- In the most basic terms the strength is **due to the cohesive forces between atoms**. In **general, high cohesive forces are related to large elastic constants, high melting points, and small coefficients of thermal expansion**.
- Figure 7-2 shows the variation of the cohesive force between two atoms as a function of the separation between these atoms.

This curve is the **resultant of the attractive and repulsive forces between the atoms.**

- The interatomic spacing of the atoms in the unstrained condition is indicated by **"$a_0$"**.
- If the crystal is subjected to a **tensile load, the separation between atoms will be increased.** The r**epulsive force decreases more rapidly with increased separation than the attractive force, so that a net force between atoms balances the tensile load**

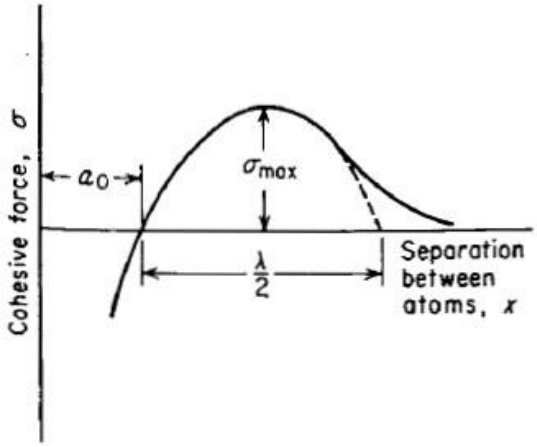


Figure 7-2 Cohesive force as a function of the separation between atoms.

- As the tensile load is increased still further, the repulsive force continues to decrease. **A point is reached where the repulsive force is negligible and the attractive force is decreasing because of the increased separation of the atoms.**

- This corresponds to the maximum in the curve, which is equal to the theoretical cohesive strength of the material.
- A good approximation to the theoretical cohesive strength can be obtained if it is assumed that the cohesive force curve can be represented by a **sine curve**.

$$\sigma = \sigma_{max} \sin \frac{2\pi x}{\lambda} \qquad (7\text{-}1)$$

- Where $\sigma_{max}$ **is the theoretical cohesive strength** and $x = a - a_0$ is the displacement in atomic spacing in a lattice with wave length "λ". For small displacements, **sin x ~ x**, and

$$\sigma = \sigma_{max} \frac{2\pi x}{\lambda} \qquad (7\text{-}2)$$

- Also, if we restrict consideration to a brittle elastic solid, then from **Hooke's law**

$$\sigma = Ee = \frac{Ex}{a_0} \qquad (7\text{-}3)$$

Eliminating x from Eqs. (7-2) and (7-3), we have

$$\sigma_{max} = \frac{\lambda}{2\pi} \frac{E}{a_0} \qquad (7\text{-}4)$$

- If we make the reasonable assumption that $a_0 \approx \lambda/2$, then

$$\sigma_{max} = E/\pi \qquad (7\text{-}5)$$

- Therefore, the potential exists for **high values of cohesive strength**.
- When fracture occurs in a brittle solid all of the work expended in producing the fracture goes into the creation of two new surfaces.
- **Each of these surfaces has a surface energy of "$\gamma_s$" J m~2**. The work done per unit area of surface in creating the fracture is the area under the stress-displacement curve.

$$U_0 = \int_0^{\lambda/2} \sigma_{max} \sin \frac{2\pi x}{\lambda} dx = \frac{\lambda \sigma_{max}}{\pi} \qquad (7\text{-}6)$$

- But this energy is equal to the energy required to create the two new fracture surfaces.

$$\frac{\lambda \sigma_{max}}{\pi} = 2\gamma_s$$

Or,

$$\lambda = \frac{2\pi\gamma_s}{\sigma_{max}} \qquad (7\text{-}7)$$

- and substituting into Eq. (7-4) gives

$$\sigma_{max} = \left(\frac{E\gamma_s}{a_0}\right)^{1/2} \qquad (7\text{-}8)$$

- Using expressions for the **force-displacement curv**e which are more **complicated than the sine-wave approximation results in estimates of $\sigma_{max}$ from E/4 to E/15**. A convenient choice is to say that ***$\sigma_{max} \approx E/10$.***
- Experience with high-strength steels shows that fracture strength in excess of 2 GPa is exceptional.
- Engineering materials typically have **fracture stresses that are 10 to 1000 times lower than the theoretical value**.
- **The only materials that approach the theoretical value are tiny, defect-free metallic whiskers and very fine-diameter silica fibers**.
- This leads to the **conclusions that laws or cracks are responsible for the lower-thanideal fracture strength of engineering materials**.

## 7-4 GRIFFITH THEORY OF BRITTLE FRACTURE

- The f**irst explanation of the discrepancy between the observed fracture strength of crystals and the theoretical cohesive strength was proposed by Griffith**.
- **Griffith's theory** in its original form is applicable only to a **perfectly brittle material** such as glass.
- However, while it cannot be applied directly to metals, **Griffith's ideas have had great influence on the thinking about the fracture of metals**.
- **Griffith proposed that a brittle materi**al contains a **population of fine cracks** which produce a **stress concentration of sufficient magnitude** so that the theoretical cohesive strength is reached in localized regions at a nominal stress which is well below the theoretical value.

- When **one of the cracks spreads into a brittle fracture**, it produces an **increase in the surface area of the sides of the crack**.
- This **requires energy to overcome the cohesive force of the atoms, or, expressed in another way, it requires an increase in surface energy**.
- The s**ource of the increased surface energy is the elastic strain energy which is released as the crack spreads**.
- **Griffith established the following criterion** for the propagation of a crack: "***A crack will propagate when the decrease in elastic strain energy is at least equal to the energy required to create the new crack surface".***
- This criterion can be used to determine the magnitude of the tensile stress which will just cause a crack of a certain size to propagate as a **brittle fracture**

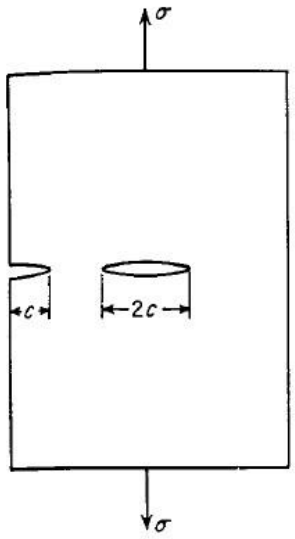


Figure 7-4 Griffith crack model

- Consider the crack model shown in Fig. 7-4. The thickness of the plate is negligible, and so the problem can be treated as one in plane stress.

- The cracks are assumed to have an elliptical shape. For a crack at the interior the length is **"2c"**, while for an edge crack it is **"c"**.
- The effect of both types of crack on the fracture behavior is the same. The stress distribution for an elliptical crack was determined by "**Inglis"**.
- A decrease in strain energy results from the formation of a crack.
- **The elastic strain energy per unit of plate thickness is equal to**

$$U_E = -\frac{\pi c^2 \sigma^2}{E} \qquad (7\text{-}12)$$

- Where **"σ"** is the tensile stress acting normal to the crack of length **"2c"**. A **negative sign is used because growth of the crack releases elastic strain energy**.
- The surface energy due to the presence of the crack is

$$U_s = 4c\gamma_s \qquad (7\text{-}13)$$

- The **total change in potential energy resulting from the creation of the crack is**

$$\Delta U = U_s + U_E \qquad (7\text{-}14)$$

- According to **Griffith's criterion**, the crack will **propagate under a constant applied stress "σ"**

- If an incremental increase in crack length produces no change in the total energy of the system; i.e., the increased surface energy is compensated by a decrease in elastic strain energy.

$$\frac{d\Delta U}{dc} = 0 = \frac{d}{dc}\left(4c\gamma_s - \frac{\pi c^2\sigma^2}{E}\right)$$

$$4\gamma_s - \frac{2\pi c\sigma^2}{E} = 0$$

$$\sigma = \left(\frac{2E\gamma_s}{\pi c}\right)^{1/2} \qquad (7\text{-}15)$$

- Equation (7-15) gives the **stress required to propagate a crack in a brittle material** as a function of the size of the microcrack.
- Note that this equation indicates that ***the fracture stress is inversely proportional to the square root of the crack length.***

Thus, **increasing the crack length by a factor of 4 reduces the fracture stress by one-half**.

- For a p**late which is thick compared with the length of the crack (plane strain) the Griffith equation is given by**

$$\sigma = \left[\frac{2E\gamma_s}{(1-\nu^2)\pi c}\right]^{1/2} \qquad (7\text{-}16)$$

- Analysis of the three-dimensional case, where the crack is a very flat oblate spheroid, results only in a modification to the constant in Griffith's equation.
- Therefore, the simplification of considering only the two-dimensional case introduces no large error.
- The Griffith's equation shows a strong dependence of fracture strength on. **"Crack length".**
- Griffith's theory satisfactorily predicts the **fracture strength of a completely brittle material such as glass.** In glass, reasonable values of crack length of about 1 μm are calculated from Eq. (7-15).
- For zinc crystals Griffith's theory predicts a critical crack length of several millimeters. This average crack length could easily be greater than the thickness of the specimen, and therefore the theory does not apply.

- **Orowan suggested** that the Griffith equation would be made more compatible with **brittle fracture in metals** by the inclusion of a term **"$\gamma_p$"** expressing the **plastic work required to extend the crack wall.**

$$\sigma_f = \left[\frac{2E(\gamma_s + \gamma_p)}{\pi c}\right]^{1/2} \approx \left(\frac{E\gamma_p}{c}\right)^{1/2} \qquad (7\text{-}17)$$

The s**urface-energy term can be neglected since estimates of the plastic-work term are about $10^2$ to $10^3$ J $m^{-2}$ compared with values of $\gamma_s$ of about 1 to 2 J $m^{-2}$.**

# FATIGUE OF METALS

## 12-1 INTRODUCTION

- It has been recognized since 1830 that a metal subjected to a repetitive or fluctuating stress will fail at a stress much lower than that required to cause fracture on a single application of load. Failures occurring under conditions of dynamic loading are called fatigue failures, presumably because it is generally observed that these failures occur only after a considerable period of service.
- Fatigue has become progressively more prevalent as technology has developed a greater amount of equipment, such as automobiles, aircraft, compressors, pumps, turbines, etc., subject to repeated loading and vibration.
- **Until today it is often stated that fatigue accounts for at least 90 percent of all service failures due to mechanical causes.**
- **Three basic factors** are necessary to **cause fatigue failure**. These are (1) **a maximum tensile stress of sufficiently high value**, (2) **a large enough variation or fluctuation in the applied stress, and** (3) **a sufficiently large number of cycles of the applied stress.**
- In addition, there are **a host of other variables, such as stress concentration, corrosion, temperature, overload, metallurgical structure, residual stresses, and combined stresses, which tend to alter the conditions for fatigue.**

## 12-2 STRESS CYCLES

- At the outset it will be advantageous to define briefly the general types of fluctuating stresses which can cause fatigue.
- Figure 12-2 serves to illustrate typical fatigue stress cycles.
- **Figure 12-2a illustrates a completely reversed cycle of stress of sinusoidal form**.
- This is an idealized situation which is produced by an R. R. Moore rotating-beam fatigue machine and which is approached in service by a rotating shaft operating at constant speed without overloads.

- **For this type of stress cycle the maximum and minimum stresses are equal**. In keeping with the conventions established in Chap. 2, the minimum stress is the lowest algebraic stress in the cycle. **Tensile stress is considered positive, and compressive stress is negative.**

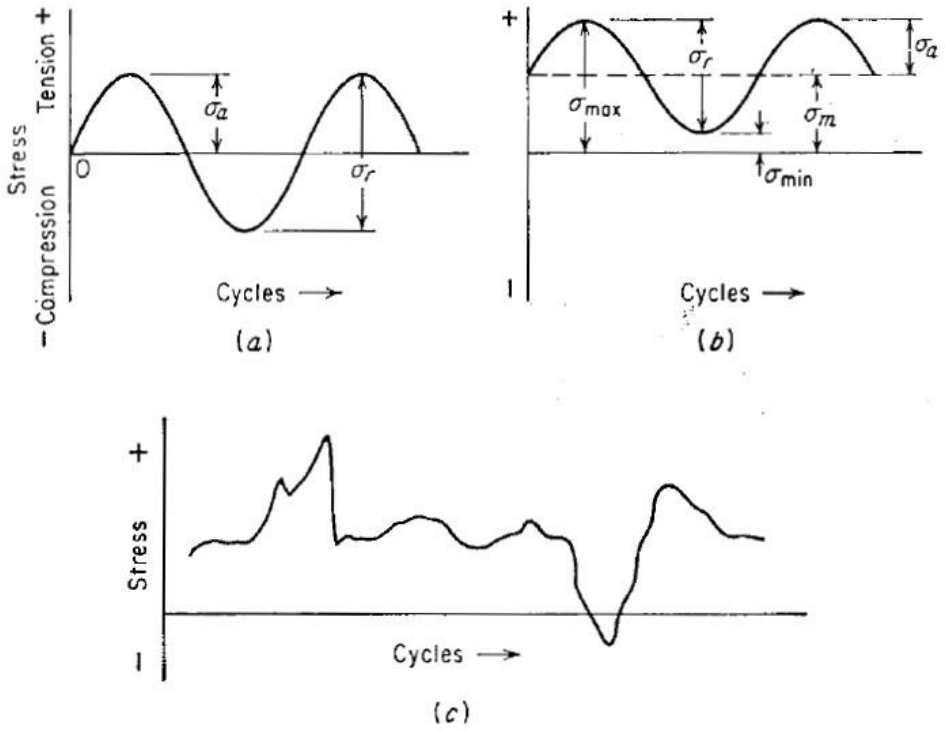


Figure 12-2 Typical fatigue stress cycles, (a) Reversed stress; (b) repeated stress; (c) irregular or random stress cycle.

- Figure 12-2b illustrates **a repeated stress cycle** in which the maximum stress $\sigma_{max}$ and minimum stress $\sigma_{min}$ are not equal.
- In this illustration they are both tension, but a repeated stress cycle could just as well **contain maximum and minimum stresses of opposite signs or both in compression**.
- Figure 12-2c illustrates a **complicated stress cycle** which might be encountered in a part **such as an aircraft wing which is subjected to periodic unpredictable overloads due to gusts.**
- A fluctuating stress cycle can be considered to be made up of two components, **a mean, or steady, stress $\sigma_m$**, and **an alternating, or variable, stress $\sigma_a$**. We must also consider the range of stress $\sigma_r$.

- As can be seen from Fig. 12-2b**, the range of stress is the algebraic difference between the maximum and minimum stress in a cycle**.

$$\sigma_r = \sigma_{max} - \sigma_{min} \qquad (12\text{-}1)$$

**The alternating stress, then, is one-half the range of stress**

$$\sigma_a = \frac{\sigma_r}{2} = \frac{\sigma_{max} - \sigma_{min}}{2} \qquad (12\text{-}2)$$

**The mean stress is the algebraic mean of the maximum and minimum stress in the cycle.**

- $$\sigma_m = \frac{\sigma_{max} + \sigma_{min}}{2} \qquad (12\text{-}3)$$

Stress ratio $$R = \frac{\sigma_{\min}}{\sigma_{\max}} \quad (12\text{-}4)$$

Amplitude ratio $$A = \frac{\sigma_a}{\sigma_m} = \frac{1 - R}{1 + R} \quad (12\text{-}5)$$

- **Two ratios are used in presenting fatigue data:**

## 12-3 THE S-N CURVE

- The basic method of presenting **engineering fatigue data** is by means of the **S-N curve**, a plot **of stress "S" against the number of cycles to failure "N"**.
- A **log scale** is almost always used for N. The value of **stress that is plotted can be $\sigma_a$, $\sigma_{max}$, or $\sigma_{min}$.**
- The **stress values are usually nominal stresses**, i.e., there is no adjustment for stress concentration.
- The **S-N relationship** is determined1 for a **specified value of $\sigma_m$, R, or A**. Most determinations of the fatigue properties of materials have been made in completed **reversed bending, where the mean stress is zero**.
- Figure 12-3 gives **typical S-N curves from rotating-beam tests**. Cases where the mean stress is not zero are of considerable engineering importance and will be considered in Sec. 12-5.
- It will be noted that this S-N curve is concerned chiefly with fatigue failure **at high numbers of cycles ($N > 10^5$ cycles)**. Under these conditions the stress, on a gross scale, is elastic, but as we shall see shortly the metal deforms plastically in a highly localized way.
- At higher stresses the fatigue life is progressively decreased, but the gross plastic deformation makes interpretation difficult in terms of stress.

For **the low-cycle fatigue region (N < $10^4$ or $10^5$ cycles)** tests are conducted with controlled cycles of elastic plus plastic strain instead of controlled load or stress cycles. Low-cycle fatigue will be considered in Sec. 12-7.

As can be seen from Fig. 12-3, **the number of cycles of stress which a metal can endure before failure increases with decreasing stress**.

- Unless otherwise indicated, N is taken as the number of cycles of stress to cause complete fracture of the specimen.
- Fatigue tests at **low stresses are usually** carried out for **$10^7$ cycles** and sometimes to- **5 * $10^8$ cycles for nonferrous metals.**
- For a few important engineering materials such **as steel and titanium, the S-N curve becomes horizontal at a certain limiting stress.**
- Below this **limiting stress, which is called the fatigue limit, or endurance limit**, the material presumably can **endure an infinite number of cycles without failure**.
- **Most nonferrous metals, like aluminum, magnesium, and copper alloys, have an S-N curve which slopes gradually downward with increasing number of cycles**.
- These **materials do not have a true fatigue limit because the S-N curve never becomes horizontal.**
- In such cases it is common practice to characterize the fatigue properties of the material by giving the **fatigue strength at an arbitrary number of cycles, for example, $10^8$ cycles**.
- **The S-N curve in the high-cycle region is sometimes described by the *Basquin equation***
- $$N\sigma_a^p = C \qquad (12\text{-}6)$$
- Where $\sigma_a$ is the stress amplitude and p and C are empirical constants.

**Determination of S – N Curves**

- The usual procedure for determining **an S-N curve is to test the first specimen at a high stress where failure is expected in a fairly short number of cycles, e.g., at about two-thirds the static tensile strength of the material**.

- The test stress is decreased for each succeeding specimen until one or two specimens do not fail in the specified numbers of cycles, which is usually at least $10^7$ cycles.

The highest stress at which a run out (non failure) is obtained is taken as the fatigue limit. For materials without a fatigue limit the test is usually terminated for practical considerations at a low stress where the life is about $10^8$ or $5 \times 10^8$ cycles.

**The S-N curve is usually determined with about 8 to 12 specimens**. It will generally be found that there is a considerable amount of scatter in the results, although a smooth curve can usually be drawn through the points without too much difficulty.

- However, if several specimens are tested at the same stress, there is a great amount of scatter in the observed values of number of cycles to failure, frequently as much as one log cycle between the minimum and maximum value.

## 12-9 STRUCTURAL FEATURES OF FATIGUE

- Studies of the basic structural changes1 that occur when a metal is subjected to cyclic stress have found **it convenient to divide the fatigue process into the following stages**:

1. **Crack initiation** - includes the early development of fatigue damage which can be removed by a suitable thermal anneal.
2. **Slip-band crack growth -** involves the deepening of the initial crack on planes of high shear stress. **This frequently is called stage I crack growth**.

- 

- 

3. **Crack growth on planes of high tensile stress** - involves growth of well-defined crack in direction normal to maximum tensile stress. **Usually called stage II crack growth**
4. **Ultimate ductile failure** - occurs when the crack reaches sufficient length so that the remaining cross section cannot support the applied load.

- The relative proportion of the total cycles to failure that are involved with each stage depends on the test conditions and the material. However, it is well established that a fatigue crack can be formed before 10 percent of the total life of the specimen has elapsed.
- There is, of course, considerable ambiguity in deciding when a deepened slip band should be called a crack. In general, larger proportions of the total cycles to failure are involved with the propagation **of stage II cracks in low-cycle fatigue than in longlife fatigue**, while **stage I crack growth comprises the largest segment for low-**

**stress, high-cycle fatigue**. If the tensile stress is high, as in the fatigue of sharply notched specimens, stage I crack growth may not be observed at all.

- The **stage I crack propagates initially along the persistent slip bands**. In a **polycrystalline metal the crack may extend for only a few grain diameters before the crack propagation changes to stage II**. The rate of crack propagation in stage I is generally very low, on the order of nm per cycle, compared with crack propagation rates of microns per cycle for stage II. The fracture surface of stage I fractures is practically featureless.
- By marked contrast the fracture surface of stage II crack propagation frequency shows a pattern of ripples or fatigue fracture striations (Fig. 12-16).
- Each striation represents the successive position of an advancing crack front that is normal to the greatest tensile stress. Each striation was produced by a single cycle of stress.
- The presence of these striations unambiguously defines that failure was produced by fatigue, but their absence does not preclude the possibility of fatigue fracture. Failure to observe striations on a fatigue surface may be due to a very small spacing that cannot be resolved with the observational method used, insufficient ductility at the crack tip to produce a ripple by plastic deformation that is large enough to be observed or obliteration of the striations by some sort of damage to the surface.
- **Since stage II cracking does not occur for the entire fatigue life**, it does not follow that counting striations will give the complete history of cycles to failure.

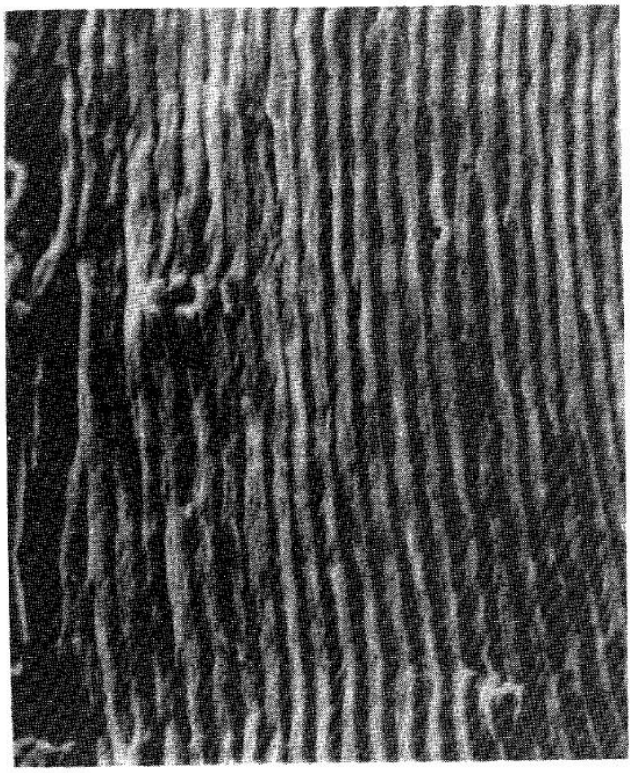

Figure 12-16 Fatigue striations in beta-annealed Ti-6A1-4V alloy

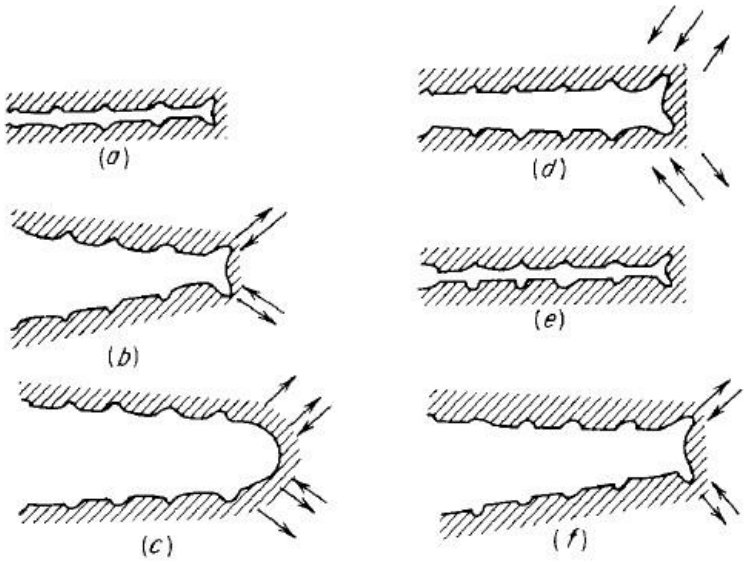


Figure 12-17 Plastic blunting process for growth of stage II fatigue crack.

- **Stage II crack propagation occurs by a plastic blunting process** that is illustrated in Fig. 12-17. At the start of the loading cycle the crack tip is sharp (Fig. 12-17a).
- As the tensile load is applied the **small double notch at the crack tip concentrates the slip along planes at 45° to the plane of the crack** (Fig. 12-l7b).

- As the crack widens to its maximum extension (Fig. 12-17c) it grows longer by plastic shearing and at the same time its tip becomes blunter. When the load is changed to compression the slip direction in the end zones is reversed (Fig. 12-11d).
- The crack faces are crushed together and the new crack surface created in tension is forced into the plane of the crack (Fig. 12-l7e) where it partly folds by buckling to form a resharpened crack tip. The resharpened crack is then ready to advance and be blunted in the next stress cycle.

## 12-10 FATIGUE CRACK PROPAGATION

- Considerable research has gone into **determining the laws of fatigue crack propagation for stage II growth**.
- Reliable **crack propagation relations permit the implementation of a fail-safe design philosophy which recognizes the inevitability of cracks in engineering structures and aims at determining the safe load and crack length which will preclude failure in a conservatively estimated service life.**
- The **crack propagation rate *"da/dN"*** is found to follow an equation

$$\frac{da}{dN} = C\sigma_a^m a^n \qquad (12\text{-}16)$$

where $C$ = a constant
$\sigma_a$ = the alternating stress
$a$ = the crack length

- In different investigations **"m"** ranges from 2 to 4 and **"n"** varies from 1 to 2.
- **Crack propagation** can also be expressed in terms of **total strain by a single powerlaw expression which extends from elastic to plastic strain region.**
- $$\frac{da}{dN} = C_1\varepsilon^{m_1} \qquad (12\text{-}17)$$

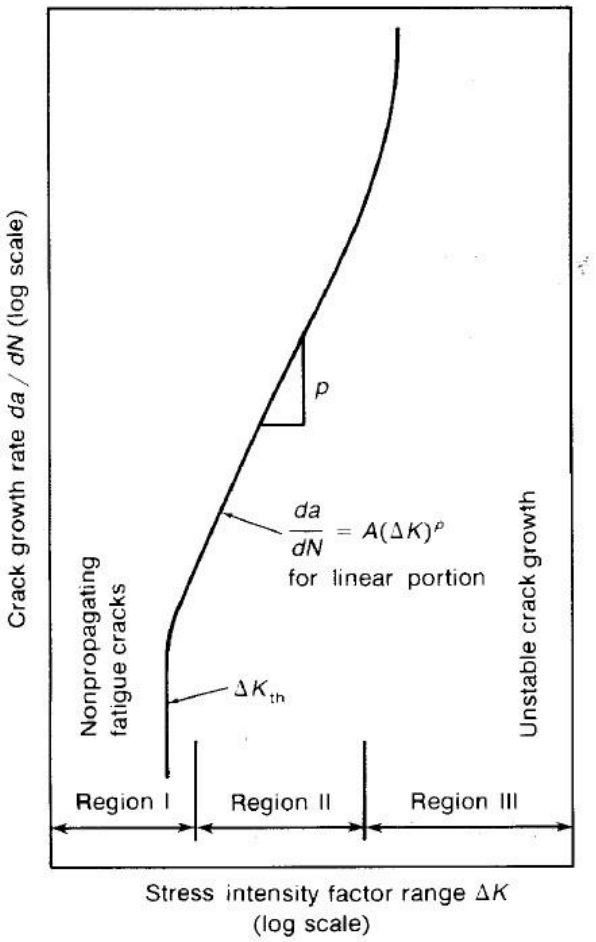


Figure 12-18 Schematic representation of fatigue crack growth behavior in a nonaggressive environment.

- The most important advance in placing **fatigue crack propagation** into a useful engineering context was the realization that **crack length versus cycles** at a series of different stress levels could be expressed by **a general plot of "*da/dN*" versus "Δ*K*"**.
- ***"da/dN"*** is the **slope of the crack growth curve** at a given value of **"σ"** and "ΔK" is the range of the stress intensity factor, defined as

$$\Delta K = K_{max} - K_{min}$$

$$\Delta K = \sigma_{max}\sqrt{\pi a} - \sigma_{min}\sqrt{\pi a} = \sigma_r\sqrt{\pi a} \qquad (12\text{-}18)$$

- Since the **stress intensity factor is undefined in compression, $K_{min}$ is taken as zero if $\sigma_{min}$ is compression.**
- The relationship between fatigue crack growth rate and AK is shown in Fig. 12-18.

**This curve has a sigmoidal shape that can be divided into *three regions*.**

- **Region I** is bounded by a ***threshold value*** $\Delta K_{th}$, **below which there is no observable fatigue crack growth.**
- At **stresses below** $\Delta K_{th}$ **cracks** behave as **non propagating cracks**. $\Delta K_{th}$ occurs at crack propagation rates of the order of 0.25 nm/cycle or less.
- **Region II** represents an essentially linear relationship between ***"log da/dN and log*** $\Delta K$***"***
- $$\frac{da}{dN} = A(\Delta K)^p \qquad (12\text{-}19)$$ :
- For this ***empirical relationship*** "p" is the slope of the curve and "A" is the value found by ***extending the straight line to*** $\Delta K = 1$ ***MPa*** $m^{1/2}$. The value of "p" is approximately ***3 for steels and in the range 3 to 4 for aluminum alloys***.
- **Equation (12-19) is often referred to as Paris' law**.
- **Region III** is a region of **accelerated crack growth**. Here $K_{max}$ **approaches** $K_c$, the **fracture toughness of the material**.
- Increasing **the mean stress in the fatigue cycle** ($R = R_{min}/R_{max} = K_{min}/K_{max}$) has a tendency ***to increase the crack growth rates*** in all portions of the ***sigmoidal curve.***
- Generally **the effect of increasing R** is **less in Region II** than in **Regions I and III**.
- The influence of R on the Paris relationship is given by

$$\frac{da}{dN} = \frac{A(\Delta K)^p}{(1-R)K_c - \Delta K} \qquad (12\text{-}20)$$

Where $K_c$= the fracture toughness applicable to the material and thickness **R**= stress ratio = $\sigma_{min}/\sigma_{max} = K_{min}/K_{max}$

- **Fatigue life testing is usually carried out under conditions of fully reversed stress or strain** ***(R = -1***).
- **However, fatigue crack growth data is usually determined for conditions of pulsating tension (R = 0).**
- **Compression loading cycles are not used because during compression loading the crack is closed and the stress intensity factor is zero**.

- While compression loading generally is considered to be of little influence in crack propagation, under variable amplitude loading compression cycles can be important.
- **Equation (12-19) provides an important link between fracture mechanics and fatigue**.
- The **elastic stress intensity factor is applicable to fatigue crack growth even in lowstrength, high ductility materials because the K values needed to cause fatigue crack growth are very low and the plastic zone sizes at the tip are small enough to permit an LEFM approach.**
- When K is known for the component under relevant loading conditions the fatigue crack growth life of the component can be obtained by integrating Eq. (12-19) between the limits of initial crack size and final crack size.

$$\Delta K = \alpha \Delta\sigma\sqrt{\pi a} = \alpha\sigma_r\sqrt{\pi a} \tag{12-21}$$

$$\frac{da}{dN} = A(\Delta K)^p = A\left(\alpha\sigma_r\sqrt{\pi a}\right)^p$$

$$= A(\alpha)^p(\sigma_r)^p(\pi a)^{p/2} \tag{12-22}$$

$$a_f = \frac{1}{\pi}\left(\frac{K_c}{\sigma_{\max}\alpha}\right)^2 \tag{12-23}$$

$$N_f = \int_0^{N_f} dN = \int_{a_i}^{a_f} \frac{da}{A(\alpha)^p(\sigma_r)^p(\pi a)^{p/2}}$$

$$= \frac{1}{A\alpha^p(\sigma_r)^p\pi^{p/2}} \int_{a_i}^{a_f} \frac{da}{a^{p/2}} \tag{12-24}$$

If $p \neq 2$,

$$\int_{a_i}^{a_f} \frac{da}{a^{p/2}} = \frac{a^{-(p/2)+1}}{-(p/2)+1}\Bigg|_{a_i}^{a_f} = \frac{a_f^{-(p/2)+1} - a_i^{-(p/2)+1}}{-(p/2)+1}$$

$$N_f = \frac{a_f^{-(p/2)+1} - a_i^{-(p/2)+1}}{(-(p/2)+1)A\sigma_r^p\pi^{p/2}\alpha^p} \tag{12-25}$$

- **Equation (12-25) is the appropriate integration of the Paris equation when $p \neq 2$** and "a" is **independent of crack length**, which unfortunately is not the usual case. For the more general case **$\alpha = f(a)$** and Eq. (12-24) must be written

$$N_f = \frac{1}{A\sigma_r^p \pi^{p/2}} \int_{a_i}^{a_f} \alpha(a)^{-p} a^{-p/2}\, da \qquad (12\text{-}26)$$

- **This is usually solved by an iterative process in which ΔK and ΔN are determined for successive increments of crack growth.**

## 12-11 EFFECT OF STRESS CONCENTRATION ON FATIGUE

- **Fatigue strength is seriously reduced** by the **introduction of a stress raiser such as a notch or hole**.
- Since actual machine elements invariably contain stress raisers like fillets, keyways, screw threads, press fits, and holes, it is not surprising to find that fatigue cracks in structural parts usually start at such geometrical irregularities.
- One of the best ways **of minimizing fatigue failure is by the reduction of avoidable stress raisers through careful design and the prevention of accidental stress raisers by careful machining and fabrication.**
- While this section is concerned with stress concentration resulting from **geometrical discontinuities, stress concentration can also arise from surface roughness** and **metallurgical stress raisers such as porosity, inclusions, local overheating in grinding, and decarburization**.
- The effect of stress raisers on fatigue is generally studied by testing specimens containing a notch, usually a **V notch or a circular notch**. It has been shown in Chap. 7 that the presence of a notch in a specimen **under uniaxial load introduces three effects**:

  **(1) There is an increase or concentration of stress at the root of the notch**

  **(2) A stress gradient is set up from the root of the notch in toward the center of the specimen**

  **(3) A triaxial state of stress is produced.**

- **The ratio of the maximum stress to the nominal stress is the theoretical stressconcentration factor $K_t$.**
- As was discussed in Sec. 2-15, values of $K_t$ can be computed from the theory of elasticity for simple geometries and can be determined from photoelastic measurements for more complicated situations. Most of the available data on stress-concentration factors have been collected by Peterson.

- **The effect of notches on fatigue strength is determined by comparing the S – N curves of notched and unnotched specimens.**
- **The data for notched specimen are usually plotted in terms of nominal stress based on the net section of the specimen.**
- **The effectiveness of the notch in decreasing the fatigue limit is expressed by the fatigue-strength reduction factor, or fatigue-notch factor, $K_f$.**
- **This factor is simply the ratio of the fatigue limit of unnotched specimens to the fatigue limit of notched specimens.**
- For materials which do not exhibit a fatigue limit the fatigue-notch factor is based on the fatigue strength at a specified number of cycles.  Values of $K_f$ have been found to vary with

**(1) Severity of the notch,**
**(2) The type of notch,**
**(3) The material,**
**(4) The type of loading, and**
**(5) The stress level.**

## 12-12 SIZE EFFECT

- An important practical problem is the prediction of the fatigue performance of large machine members from the results of laboratory tests on small specimens.
- Experience has shown that in **most cases a size effect exists**; i.e., the fatigue strength of large members is lower than that of small specimens.
- A precise study of this effect is difficult for several reasons. It is extremely difficult, if not altogether impossible, to prepare geometrically similar specimens of increasing diameter which have the same metallurgical structure and residual stress distribution throughout the cross section.
- **The problems in fatigue testing large-sized specimens are considerable, and there are few fatigue machines which can accommodate specimens having a wide range of cross sections**.
- Changing the size of a fatigue specimen usually results in a variation in **two factors**.

(1) First, increasing the diameter increases the volume or surface area of the specimen. The change in amount of surface is of significance, since fatigue failures usually start at the surface.

(2) Second, for plain or notched specimens loaded in bending or torsion, an increase in diameter usually decreases the stress gradient across the diameter and increases the volume of material which is highly stressed.

- **Analysis of considerable data for steels has shown a size-effect relationship between fatigue limit and the critically stressed volume of the material**.

- $$\sigma_{f1} = \sigma'_{f0}\left(\frac{V}{V_0}\right)^{-0.034} \qquad (12\text{-}29)$$

- Where **"$\sigma_{f1}$" is the fatigue limit for a critical volume V** and **"$\sigma_{f0}$" is the known fatigue limit for a specimen with volume $V_0$**.

- **Critically stressed volume** is defined **as the volume near the surface of the specimen**

**that is stressed to at least 95 percent of $\sigma_{max}$**.

## 12-13 SURFACE EFFECTS AND FATIGUE

- Practically all fatigue failures start at the surface. For many common types of loading, like bending and torsion, the maximum stress occurs at the surface so that it is logical that failure should start there.

- **However, in axial loading the fatigue failure nearly always begins at the surface**. **There is ample evidence that fatigue properties are very sensitive to surface condition**.

- **The factors which affect the surface of a fatigue specimen can be divided roughly into three categories**,

(1) Surface roughness or stress raisers at the surface, (2)
Changes in the fatigue strength of the surface metal, and
(3) Changes in the residual stress condition of the surface.

- In addition, the surface is subjected to **oxidation and corrosion**.

**Table 12-3 Fatigue life of SAE 3130 steel specimens tested under completely reversed stress at 655 MPa†**

| Type of finish | Surface roughness, $\mu$m | Median fatigue life, cycles |
|---|---|---|
| Lathe-formed | 2.67 | 24,000 |
| Partly hand-polished | 0.15 | 91,000 |
| Hand-polished | 0.13 | 137,000 |
| Ground | 0.18 | 217,000 |
| Ground and polished | 0.05 | 234,000 |
| Superfinished | 0.18 | 212,000 |

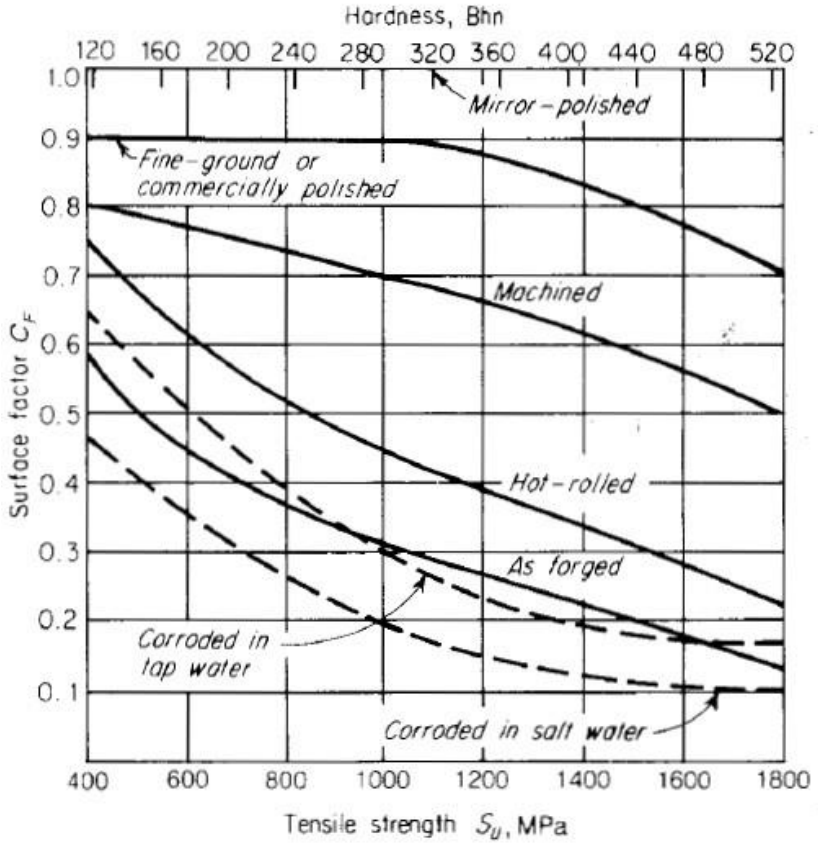


Figure 12-20 Reduction factor for fatigue limit of steel due to various surface treatments.

**Surface Roughness**

- Since the early days of fatigue investigations, it has been recognized that different surface finishes produced by different machining procedures can appreciably affect fatigue performance. Smoothly polished specimens, in which the fine scratches (stress raisers) are oriented parallel with the direction of the principal tensile stress, give

the highest values in fatigue tests. Such carefully polished specimens are usually used in laboratory fatigue tests and are known as **"par bars."**

- Table 12-3 **indicates how the fatigue life of cantilever-beam specimens varies with the type of surface preparation**. Extensive data on this subject have been published by ***Siebel and Gaier***.
- Figure 12-20 shows the influence **of various surface finishes on steel in reducing the fatigue limit of carefully polished "par bars.**" Note that the surface finish is characterized by the process used to form the surface.
- **The extreme sensitivity of high-strength steel to surface conditions is well illustrated**.

**Changes in Surface Properties**

- Since **fatigue failure** is so dependent on the condition of **the surface, anything that changes the fatigue strength of the surface material will greatly alter the fatigue properties.**
- **Decarburization of the surface of heat-treated** steel is particularly **detrimental** to fatigue performance.
- Similarly, **the fatigue strength of aluminum alloy sheet is reduced when a soft aluminum coating is applied to the stronger age-hardenable aluminum-alloy sheet.**
- **Marked improvements in fatigue properties can result from the formation of harder and stronger surfaces on steel parts by carburizing and nitriding.**
- However, **since favorable compressive residual stresses are produced in the surface by these processes, it cannot be considered that the higher fatigue properties are due exclusively to the formation of higher-strength material on the surface.**
- The effectiveness of carburizing and nitriding in improving fatigue performance is greater for cases where a high stress gradient exists, as in bending or torsion, than in an axial fatigue test. The greatest percentage increase in fatigue performance is found when notched fatigue specimens are nitrided.
- **The amount of strengthening depends on the diameter of the part and the depth of surface hardening. Improvements in fatigue properties similar to those**

**caused by carburizing and nitriding may also be produced by flame hardening and induction hardening.**

- It is a general characteristic of **fatigue in surface-hardened parts that the failure initiates at the interface between the hard case and the softer case, rather than at the surface**.

**Surface Residual Stress**

- **The formation of a favorable compressive residual-stress pattern at the surface is probably the most effective method of increasing fatigue performance**.
- It can be considered that residual stresses are locked-in stresses which are present in a part which is not subjected to an external force.
- Only macrostresses, which act over regions which are large compared with the grain size, are considered here.
- They can be measured by x-ray methods or by noting the changes in dimensions when a thin layer of material is removed from the surface.
- **Residual stresses arise when plastic deformation is not uniform throughout the entire cross section of the part being deformed**.
- The **chief commercial methods of introducing favorable compressive residual stresses in the surface are by surface rolling with contoured rollers and by shot peening.**
- **Although some changes in the strength of the metal due to strain hardening occur during these processes, the improvement in fatigue performance is due chiefly to the formation of surface compressive residual stress.**
- Surface rolling is particularly adapted to large parts. It is frequently used in critical regions such as the fillets of crankshafts and the bearing surface of railroad axies.
- **Shot peening consists in projecting fine steel or cast-iron shot against the surface at high velocity**.

It is **particularly adapted to mass-produced parts of fairly small size**. The severity of the stress produced by shot peening is frequently controlled by measuring the residual deformation of shot-peened beams called Almen strips.

## CREEP AND STRESS RUPTURE

• In several previous chapters it has been mentioned that the strength of metals decreases with increasing temperature. Since the mobility of atoms increases rapidly

with temperature, it can be appreciated that diffusion-controlled processes can have a very significant effect on high-temperature mechanical properties.

- **High temperature** will also result in **greater mobility of dislocations** by the mechanism of **climb**. The equilibrium concentration of vacancies likewise increases with temperature. New deformation mechanisms may come into play at elevated temperatures.
- In some metals the slip system changes, or additional slip systems are introduced with increasing temperature.
- Deformation at grain boundaries becomes an added possibility in the high-temperature deformation of metals.
- Another important factor to consider is the effect of prolonged exposure at elevated temperature on the metallurgical stability of metals and alloys.
- For example, **cold-worked metals will recrystallize and undergo grain coarsening**, while age-hardening alloys may overage and lose strength as the second-phase particles coarsen.
- **Another important consideration is the interaction of the metal with its environment at high temperature**.
- **Catastrophic oxidation and intergranular penetration of oxide must be avoided.**

**Examples:**

- For a long time the principal high-temperature applications were associated with steam power plants, oil refineries, and chemical plants. The operating temperature in equipment such as boilers, steam turbines, and cracking units seldom exceeded $500^0$C.
- With the introduction of the gas-turbine engine, requirements developed for materials to operate in critically stressed parts, like turbine buckets, at temperatures around $800^0$C.
- The design of more powerful engines has pushed this limit to around $1000^0$C.
- Rocket engines and ballistic-missile nose cones present much greater problems, which can be met only by the most ingenious use of the available high-temperature materials and the development of still Better ones.
- There is no question that the available materials of construction limit rapid advancement in high-temperature technology.

**Time dependent deformation:**

- An important characteristic of **high-temperature strength** is that it must always be considered with respect to some time scale.
- The tensile properties of most engineering metals at room temperature are independent of time, for practical purposes.
- It makes little difference in the results if the loading rate of a tension test is such that it requires 2 h or 2 min to complete the test.
- However, at elevated temperature the strength becomes very dependent on both strain rate and time of exposure.
- **A number of metals under these conditions behave in many respects like viscoelastic materials**. A metal subjected to a constant tensile load at an elevated temperature will creep and undergo a time-dependent increase in length.

**Advantages of Homologous temperature:**

- **A strong time dependence of strength becomes important in different materials at different temperatures**. What is high temperature for one material may not be so high for another.
- To compensate for this, temperature often is expressed **as a homologous temperature**,
i.e., **the ratio of the test temperature to the melting temperature on an absolute temperature scale**.
- **Generally, creep becomes of engineering significance at a homologous temperature greater than 0.5.**
- The tests which are used to measure elevated-temperature strength must be selected on the basis of the time scale of the service which the material must withstand.
- Therefore, special tests are required to evaluate the performance of materials in different kinds of high-temperature service.
- The creep test measures the dimensional changes which occur from elevatedtemperature exposure, while the stress rupture test measures the effect of temperature on the long-time load-bearing characteristics.

## 13-2 TIME-DEPENDENT MECHANICAL BEHAVIOR

- Before proceeding with a discussion of high-temperature mechanical behavior we shall digress to consider time-dependent mechanical behavior in a more general context.
- **Creep is one important manifestation of anelastic behavior**.
- In metals anelastic effects usually are very small at room temperature, but they can be large in the same temperature region for polymeric materials.
- A second material behavior discussed in this section is internal friction, which arises from a variety of anelastic effects in crystalline solids.
- **However, under certain circumstances there is time dependence to elastic strain which is called anelasticity**.
- In Fig. 13-1, an elastic strain is applied to an anelastic material. With increasing time the strain gradually increases to a value $e_2$, the completely relaxed strain.
- The amount of anelastic strain is $e_1 - e_2$ If the load is suddenly removed at $t = t_1$ the material undergoes an immediate elastic contraction equal in magnitude to $e_1$ and with the passage of time the strain decays to zero. This behavior is known as an ***elastic aftereffect***.
- If a rod of material is loaded to an elastic stress so rapidly that there is not time for any thermal effects to equilibrate with the surroundings, the loading is done at constant entropy and under adiabatic conditions. For uniaxial loading the change in temperature of the material with strain is given by

$$\left.\frac{\partial T}{\partial \varepsilon}\right|_s = -\frac{V_m \alpha E T}{c_v} \qquad (13\text{-}1)$$

where $V_m$ = the molar volume of the material
$\alpha$ = the coefficient of linear thermal expansion
$E$ = the isothermal Young's modulus
$T$ = the absolute temperature
$c_v$ = the specific heat at constant volume

- Since a is positive for most materials and the other terms in Eq. (13-1) are also positive, it follows that an adiabatic elastic tension lowers the temperature of the material and an adiabatic compression increases the temperature. However, these temperature changes associated with the thermoelastic effect are usually small.

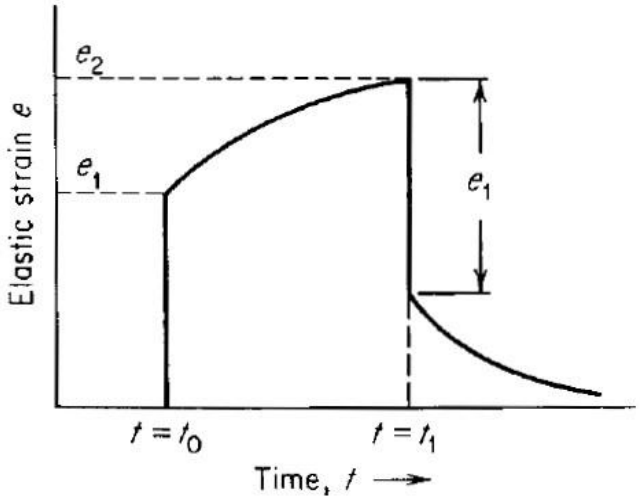


Figure 13-1 Anelastic behavior and the elastic after - effect.

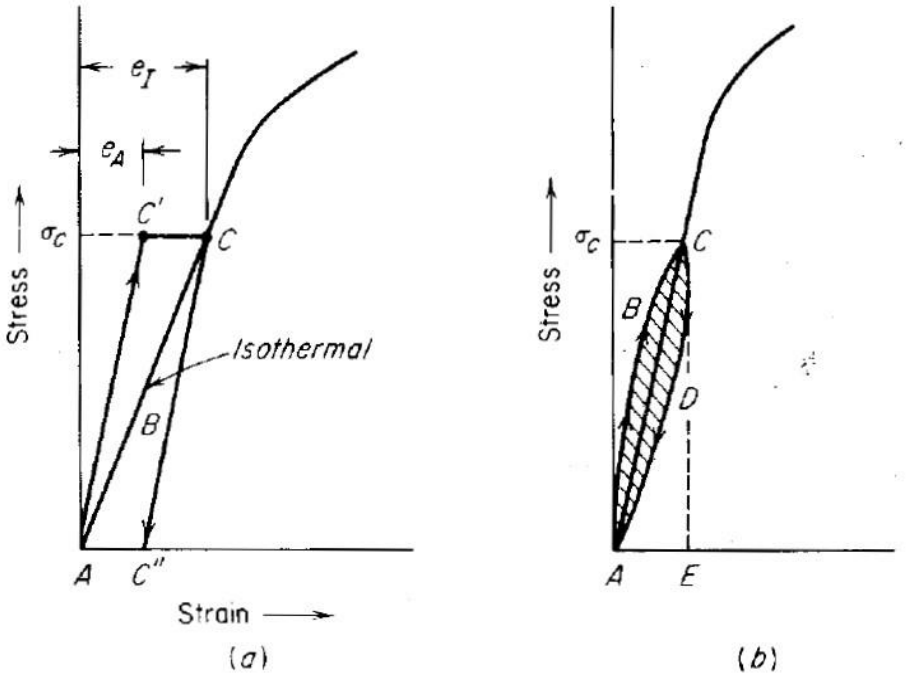


Figure 13-2 (a) Idealized adiabatic and isothermal stress-strain curves; (b) elastic hysteresis loop.

## 13-3 THE CREEP CURVE

- The **progressive deformation of a material at constant stress is called creep**.

To determine **the engineering creep curve of a metal, a constant load is applied to a tensile specimen maintained at a constant temperature, and the strain (extension) of the specimen is determined as a function of time.**

- Although the measurement of creep resistance is quite simple in principle, in practice it requires considerable laboratory equipment.
- **Curve A** in Fig. 13-4 illustrates the **idealized shape of a creep curve**.
- **The slope of this curve ($d\varepsilon/dt$ or $\dot{\varepsilon}$) is referred to as the creep rate**.
- Following **an initial rapid elongation of the specimen**, $\varepsilon_0$, the creep rate decreases with time, then reaches essentially a steady state in which the creep rate changes little with time, and finally the creep rate increases rapidly with time until fracture occurs.
- Thus, it is natural to discuss the creep curve in terms of its **three stages**.
- It should be noted, however, that the degree to which these three stages are readily distinguishable depends strongly on the applied stress and temperature.

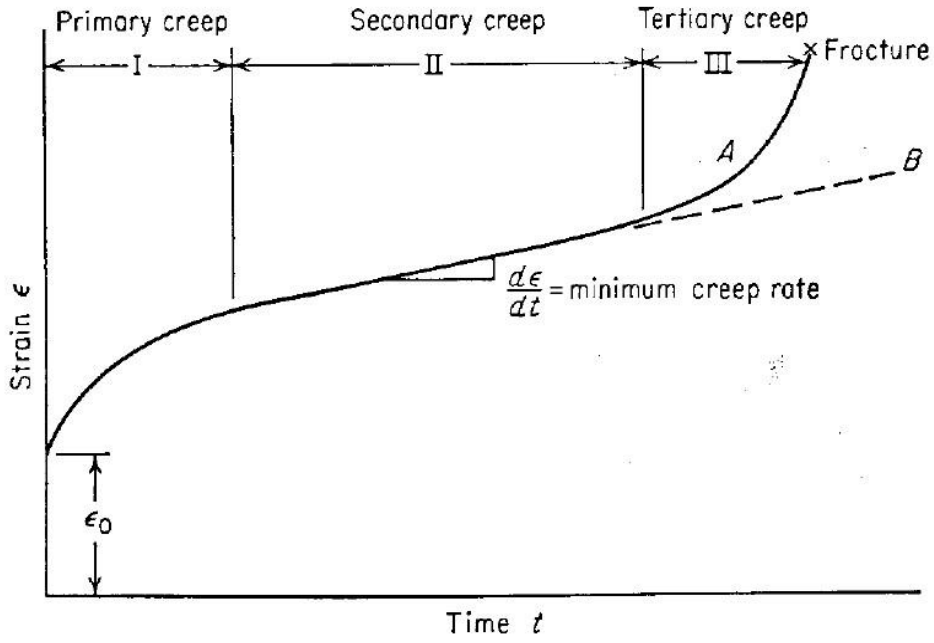


Figure 13-4 Typical creep curve showing the three steps of creep. Curve A, constant-load test; curve B, constant-stress test.

- In making an engineering creep test, it is usual practice to maintain the load constant throughout the test.

- Thus, as the specimen elongates and decreases in cross-sectional area, the axial stress increases.

The initial stress which was applied to the specimen is usually the reported value of stress. Methods of compensating for the change in dimensions of the specimen so as to carry out the creep test under constant-stress conditions have been developed.

- When **constant-stress tests are made it is found that the onset of stage III is greatly delayed.**
- The dashed line **(curve B)** shows the shape of **a constant-stress creep curve.**
- In engineering situations it is usually the load not the stress that is maintained constant, so a constant-load creep test is more important.
- However, fundamental studies of the mechanism of creep should be carried out under constant-stress conditions.

**Andrade's Creep Curve:**

- Andrade's pioneering work on creep has had considerable influence on the thinking on this subject.
- He considered that the constant-stress creep curve represents the superposition of two separate creep processes which occur after the sudden strain which results from applying the load.
- The first component of the creep curve is a transient creep with a creep rate decreasing with time. Added to this is a constant-rate viscous creep component.
- The **superposition of these creep processes** is shown in Fig. 13-5.
- Andrade found that the creep curve could be represented by the following empirical equation:

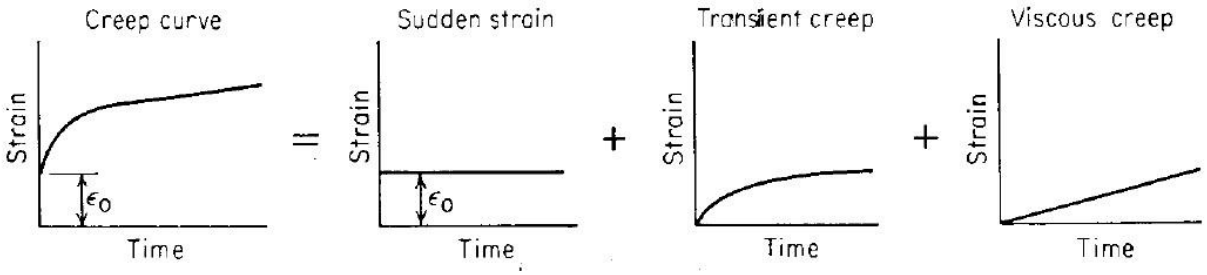


Figure 13-5 Andrade's analysis of the competing processes which determine the creep curve

$$\varepsilon = \varepsilon_0\left(1 + \beta t^{1/3}\right)e^{(\kappa t)} \qquad (13\text{-}8)$$

Where $\varepsilon$ is the strain in time t and $\beta$and k are constants.

- The transient creep is represented by $\beta$ and Eq. (13-8) reverts to this form when k = 0.

The constant k describes an extension per unit length which proceeds at a constant rate.

- An equation which gives better fit than Andrade's equation, although it has been tested on a limited number of materials, was proposed by Garofalo.

- $$\varepsilon = \varepsilon_0 + \varepsilon_t\left(1 - e^{-rt}\right) + \dot{\varepsilon}_s t \qquad (13\text{-}9)$$

where $\varepsilon_0$ = the instantaneous strain on loading
$\varepsilon_t$ = the limit for transient creep
$r$ = the ratio of transient creep rate to the transient creep strain
$\dot{\varepsilon}_s$ = the steady-state creep rate

- The various stages of the creep curve shown in Fig. 13-4 require further explanation. It is generally considered in this country that the creep curve has three stages.
- In British terminology the instantaneous strain designated by $\varepsilon_0$in Fig. 13-4 is often called the first stage of creep, so that with this nomenclature the creep curve is considered to have four stages.
- The strain represented by $\varepsilon_0$ occurs practically instantaneously on the application of the load. Even though the applied stress is below the yield stress, not all the instantaneous strain is elastic.
- Most of this strain is instantly recoverable upon the **release of the load (elastic),** while part is **recoverable with time (anelastic)** and the rest is nonrecoverable (plastic).
- Although the instantaneous strain is not really creep, it is important because it may constitute a considerable fraction of the allowable total strain in machine parts.
- Sometimes the instantaneous strain is subtracted from the total strain in the creep specimen to give the strain due only to creep. This type of creep curve starts at the origin of coordinates.

## Three Stages of Creep:

**Primary Creep:**

- **The first stage of creep**, known as ***primary creep***, represents a **region of decreasing creep rate**.
- **Primary creep** is a period of **predominantly transient creep** in which the **creep resistance of the material increases by virtue of its own deformation.**

For low temperatures and stresses, as in the creep of lead at room temperature, primary creep is the predominant creep process.

**Secondary Creep:**

- The **second stage of creep**, known also as ***secondary creep***, is a **period of nearly constant creep rate which results from a balance between the competing processes of strain hardening and recovery.**
- For this reason, secondary creep is usually referred to as steady-state creep. The average value of the creep rate during secondary creep is called the minimum creep rate.

**Tertiary Creep:**

- **Third-stage or tertiary creep** mainly **occurs in constant-load creep tests at high stresses at high temperatures.**
- **Tertiary creep occurs when there is an effective reduction in cross-sectional area either because of necking or internal void formation.**
- **Third-stage creep is often associated with metallurgical changes such as coarsening of precipitate particles, recrystallization, or diffusion changes in the phases that are present.**

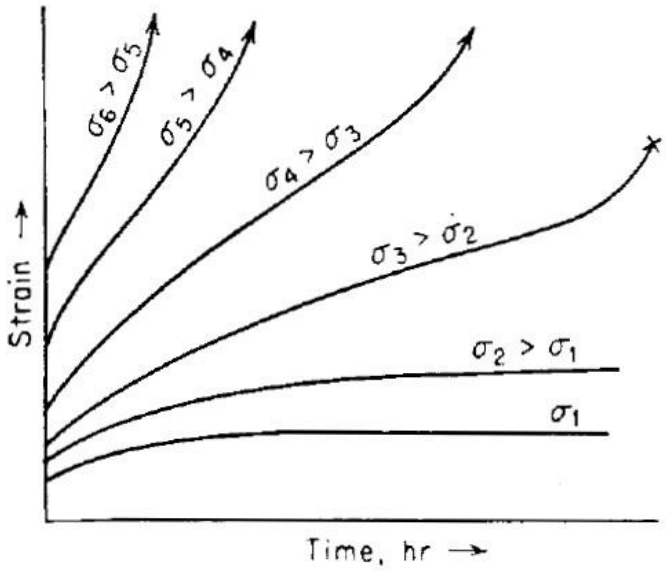


Figure 13-6 Schematic representation "of the effect of stress on creep curves at constant temperature.

- **Figure 13-6 shows the effect of applied stress on the creep curve at constant temperature**.
- It is apparent that **a creep curve with three well-defined stages will be found for only certain combinations of stress and temperature.**
- A similar family of curves is obtained for creep at constant stress for different temperatures.
- **The higher the temperature, the greater the creep rate.**

## 13-4 THE STRESS-RUPTURE TEST

- **The stress-rupture test is basically similar to the creep test except** that the test is always carried out to the failure of the material
- **Higher loads are used with the stress-rupture test than in a creep test**, and therefore the creep rates are higher.
- **Ordinarily the creep test is carried out at relatively low stresses so as to avoid tertiary creep**. Emphasis in the creep test is on precision determination of strain, particularly as to the determination of the minimum creep rate.
- **Creep tests are frequently conducted for periods of 2,000 h and often to 10,000 h.**
- In the creep test the total strain is often less than 0.5 percent, while in the stress-rupture test the total strain may be around 50 percent.
- Thus, simpler **strain-measuring devices, such as dial gages, can be used**.
- Stress-rupture equipment is simpler to build, maintain, and operate than creep-testing equipment, and therefore it lends itself more readily to multiple testing units.
- The **higher stresses and creep rates of the stress-rupture test cause structural changes to occur in metals at shorter times than would be observed ordinarily in the creep test, and therefore stress-rupture tests can usually be terminated in 1,000 h**.
- The basic information obtained from the stress-rupture test is the time to cause failure at a given nominal stress for a constant temperature.
- The elongation and reduction of area at fracture are also determined. If the test is of suitable duration, it is customary to make elongation measurements as a function of time and from this to determine the minimum creep rate.
- **The stress is plotted against the rupture time on a log-log scale (Fig. 13-7). A straight line will usually be obtained for each test temperature.**
- **Changes in the slope of the stress-rupture line are due to structural changes occurring in the material, e.g., changes from transgranular to intergranular fracture, oxidation, recrystallization and grain growth, or other structural changes such as spheroidization, graphitization, or sigma-phase formation.**
- It is important to know about the existence of such instabilities, since serious errors in extrapolation of the data to longer times can result if they are not detected.

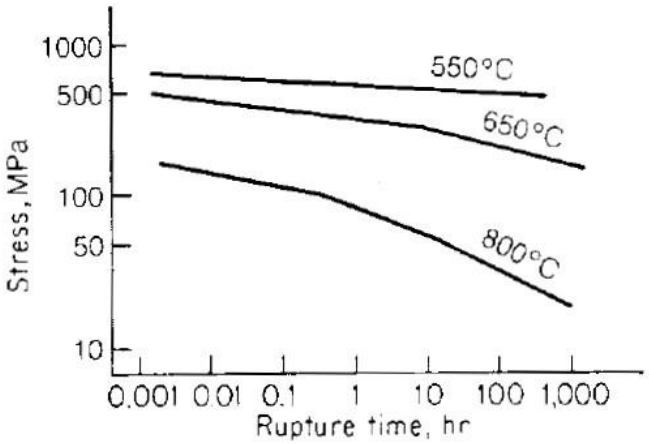


Figure 13-7 Method of plotting stress-rupture data (schematic)

## 13-7 DEFORMATION MECHANISM MAPS

- A practical way of illustrating and **utilizing the constitutive equations for the various creep deformation mechanisms is with deformation mechanism maps.**
- **Ashby and co-workers have developed these maps in stress-temperature space.**
- The various regions of the map (Fig. 13-11) indicate the dominant deformation mechanism for that stress-temperature combination.
- The boundaries of these regions are obtained by equating the appropriate equations in Sec. 13-6 and solving for stress as a function of temperature.
- The boundaries represent combinations of stress and temperature where the respective strain rates for the two deformation mechanisms are equal.

We see for example, for the metal shown in Fig. 13-11 **that at a homologous temperature of 0.8** and **a low stress the deformation occurs by diffusional low** (Nabarro-Herring creep).

- **Keeping the temperature constant and increasing the stress we enter a region of power-law creep (dislocation creep) and at still higher stress the metal deforms by thermally activated dislocation glide.**
- **The upper bound on the diagram is the stress to produce slip in a perfect (dislocation free) lattice.**

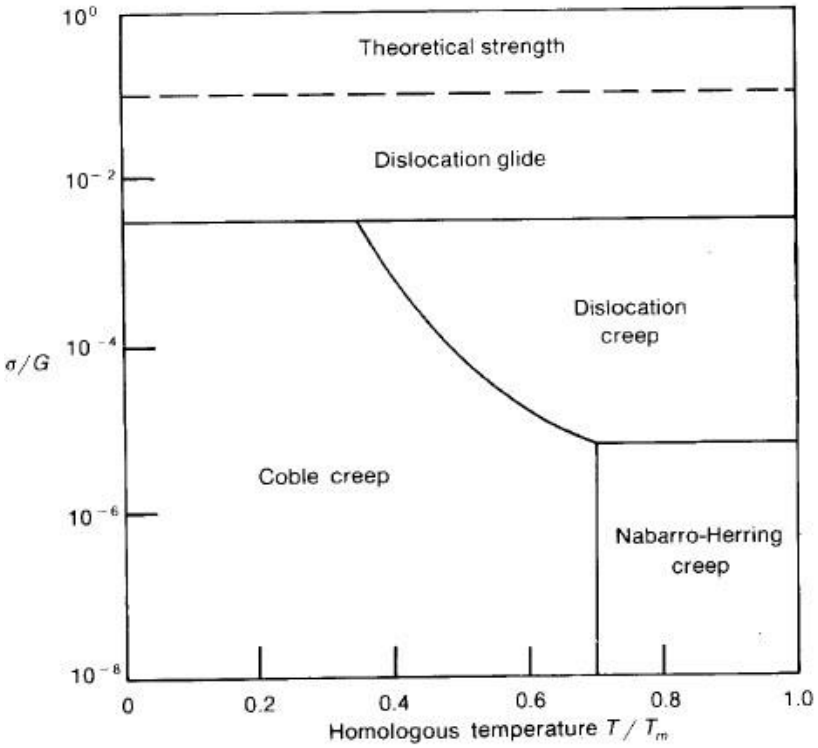


Figure 13-11 Simplified deformation mechanism map. (After Ashby.)

- Contours of isostrain rate can be calculated from the constitutive equations and plotted on the deformation mechanism map (Fig. 13-12).
- Thus, in addition to identifying the dominant deformation mechanism the map allows selection of any two of the three variables, a, £, or T, and establishment of the third value.
- **A deformation mechanism map is not only a useful pedagogical tool but it can be helpful in decisions involving alloy design and selection.**

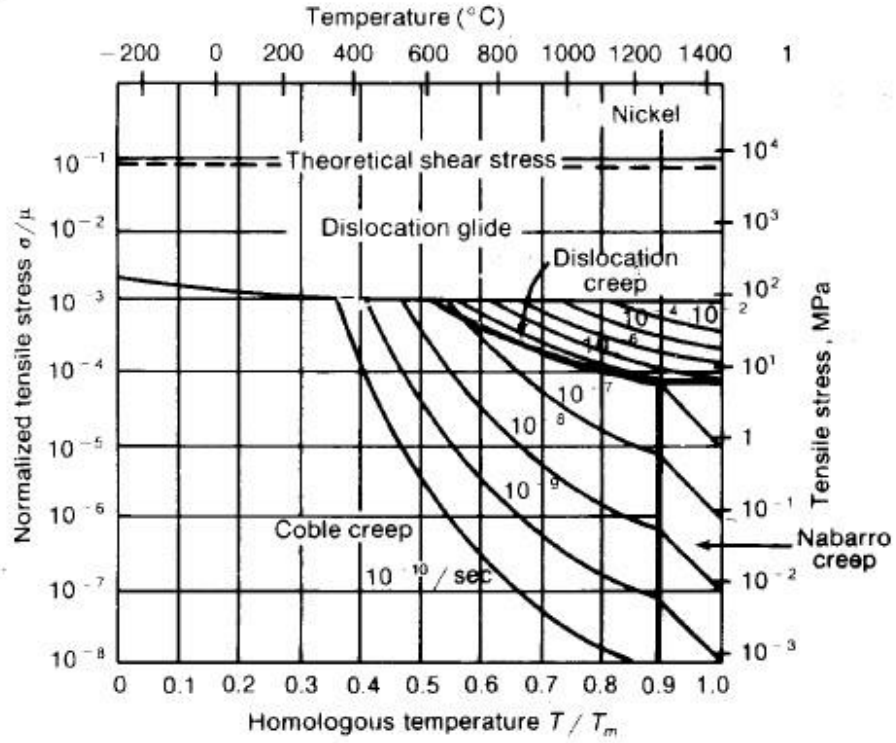


Figure 13-12 Deformation mechanism map for pure nickel with grain size of 32 μm. *(M. F. Ashby, Acta Met., vol. 20, p. 3, 1972.)*

## 13-9 SUPERPLASTICITY

- **Superplasticity is the ability of a material to withstand very large deformations in tension without necking.**
- **Elongations in excess of 1,000 percent are observed.**
- In Sec. 8-6 we showed **that superplasticity was related to the existence of a high strain-rate sensitivity.**
- In this section we deal more broadly with superplastic behavior and relate it to the appropriate high-temperature deformation mechanisms.
- **Superplastic behavior occurs at $T > 0.5T_m$.** Not only does the material show large extensibility without fracture but at low strain rates the flow stress is very low.
- **Thus, complex shapes may be readily formed under superplastic conditions. The requirements for a material to exhibit superplasticity are a fine grain size (less**

- **than 10 μm) and the presence of a second phase which inhibits grain growth at the elevated temperature.**

Most superplastic alloys are eutectic or eutectoid compositions. The strength of the second phase should be similar to that of the matrix phase to avoid extensive internal cavity formation.

## NON-DESTRUCTIVE TESTING (NDT)

**Why use NDT?**

- Components are not destroyed
- Can test for internal flaws
- Useful for valuable components
- Can test components that are in use

1. **Penetrant testing**
   - Used for surface flaws.
   - The *oil and chalk* test is a traditional version of this type of testing. Colored dyes are now used.

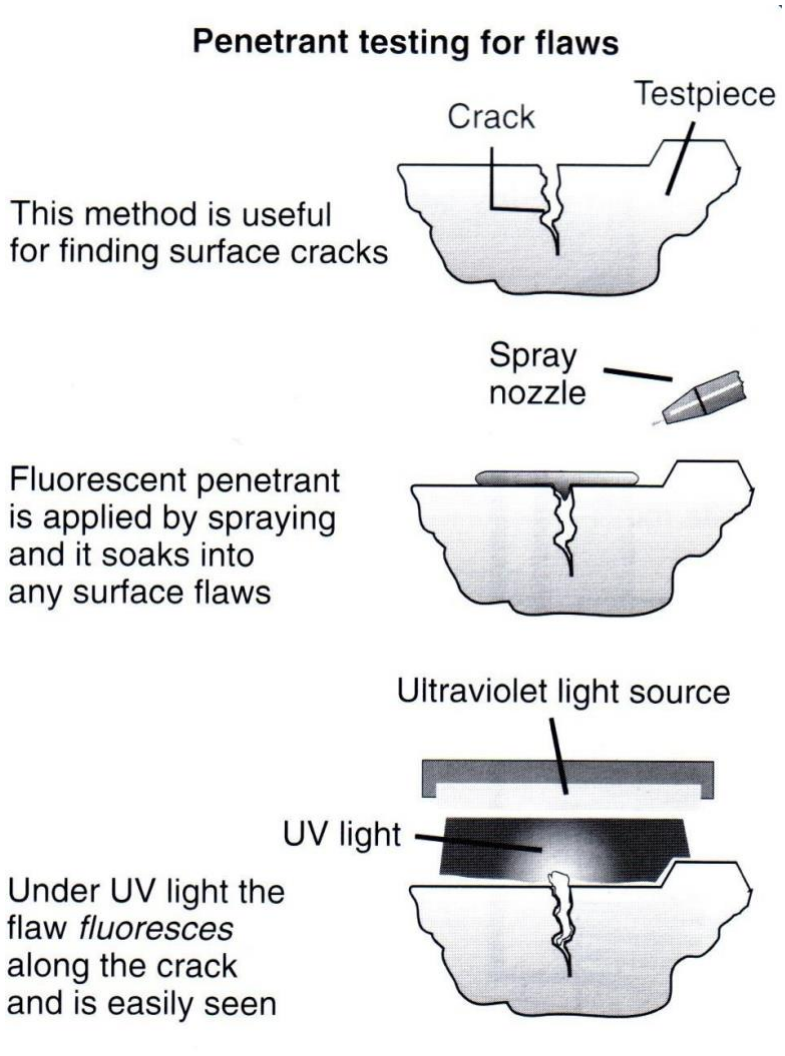


2. **Magnetic particle testing**
   - Used for ferrous metals.
   - Detects flaws close to the surface of the material.

- The component to be tested must first be magnetized.

Magnetic particles which can be dry or in solution are sprinkled onto the test piece.

- The particles stick to the magnetic field and flaws can be inspected visually by examining the pattern to see if it has been distorted.
- The component must be demagnetized after testing.

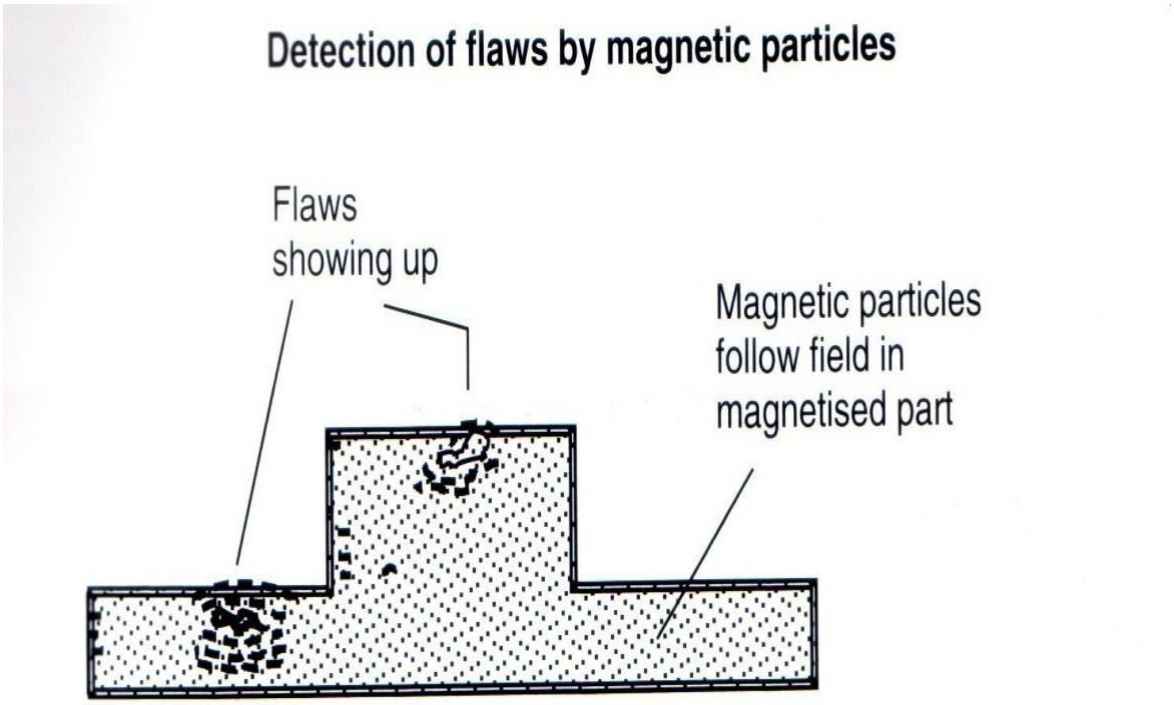


Flaws which are near the surface are more likely to be detected because the distorted magnetic field shows up in the magnetic particle pattern

**3. Eddy current testing**

- Used for non-ferrous metals
- A.C. current is passed through the coil.
- The test piece is passed under the coil causing secondary currents called eddy currents to flow through the test piece. This causes a magnetic field to flow in the test piece.
- The flaws are detected on an oscilloscope by measuring a change in the magnetic field.

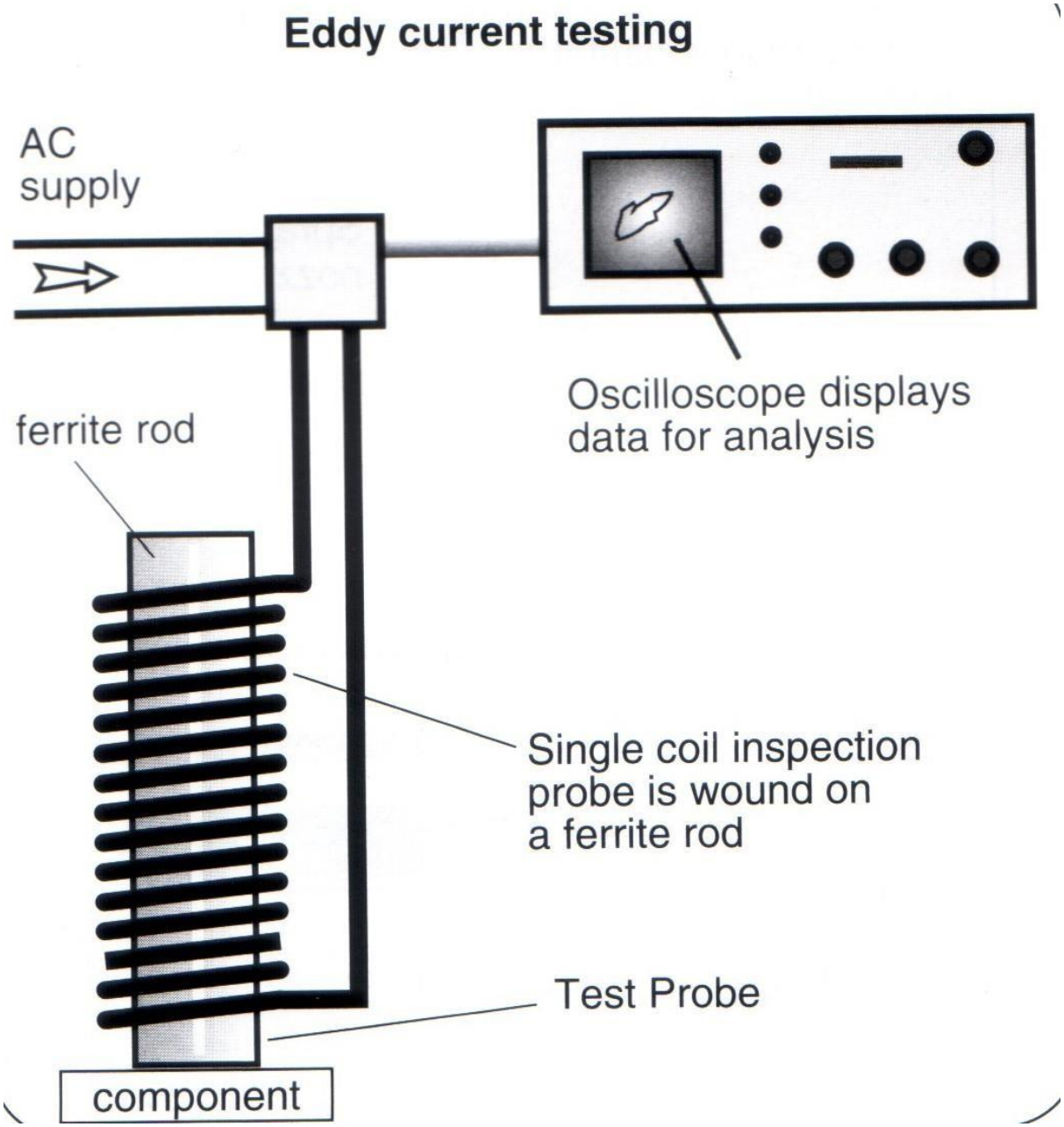


**4. Ultrasonic testing**

Ultrasonic Sound waves are bounced off the component and back to a receiver. If there is a change in the time taken for the wave to return this will show a flaw. This is similar to the operation of a sonar on a ship.

**Operation.**

- The ultrasonic probe sends the sound wave through the piece.
- The sound waves bounces off the piece and returns.
- The results are then placed on the display screen in the form of peaks.

- Where the peaks fluctuate this will show a fault in the piece.

**Uses.**

- This is generally used to find internal flaws in large forgings, castings and in weld inspections.

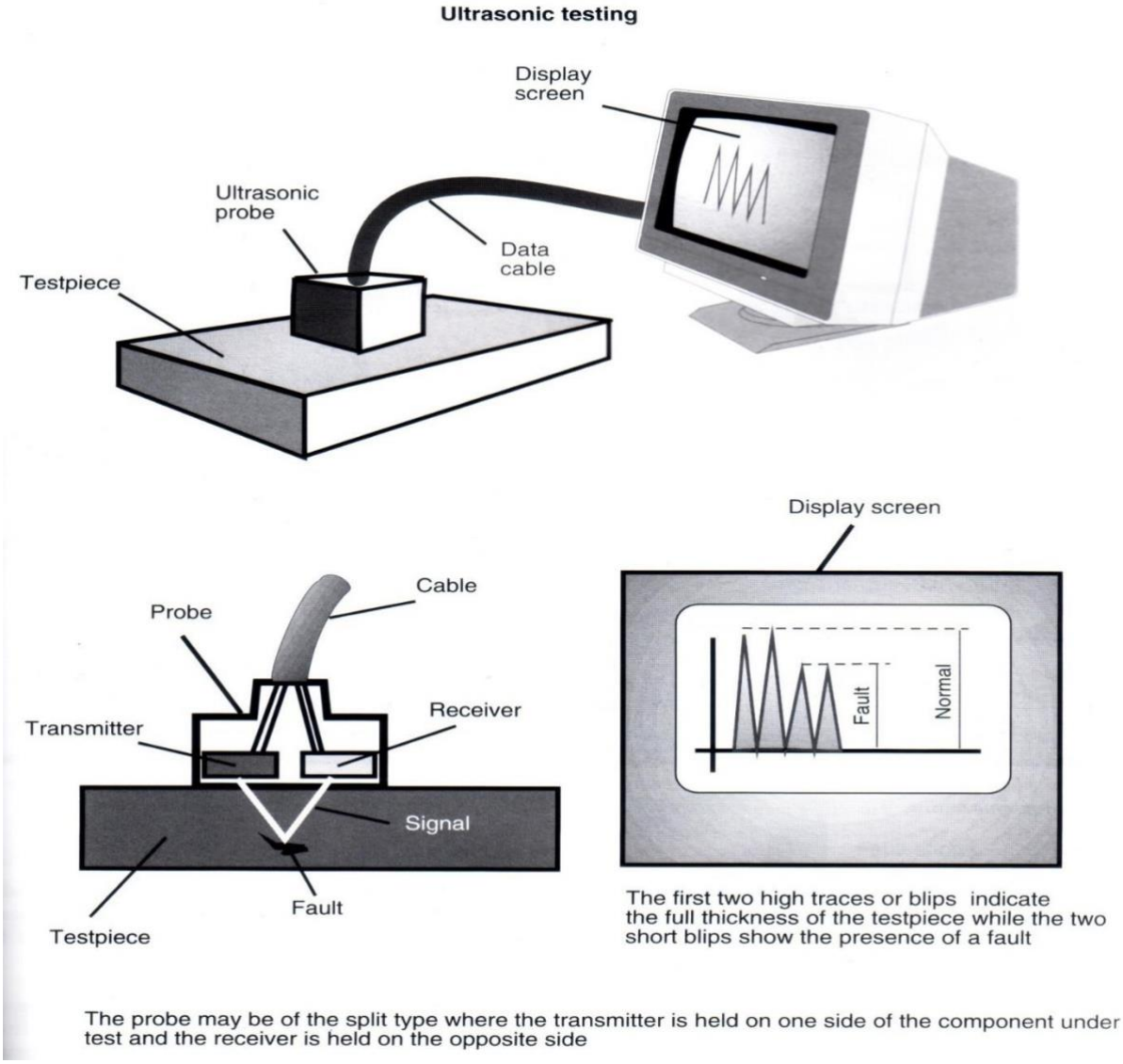

□

**5. Radiography (X-ray) Testing**

- The x-ray are released by heating the cathode.
- They are then accelerated by the D.C. current and directed onto the piece by the tungsten anode.
- The x-rays then pass through the test piece onto an x-ray film which displays the results.
- The x-rays cannot pass through the faults as easily making them visible on the x-ray film.

**Uses.**

- This is a test generally used to find internal flaws in materials. It is used to check the quality of welds, for example, to find voids or cracks.

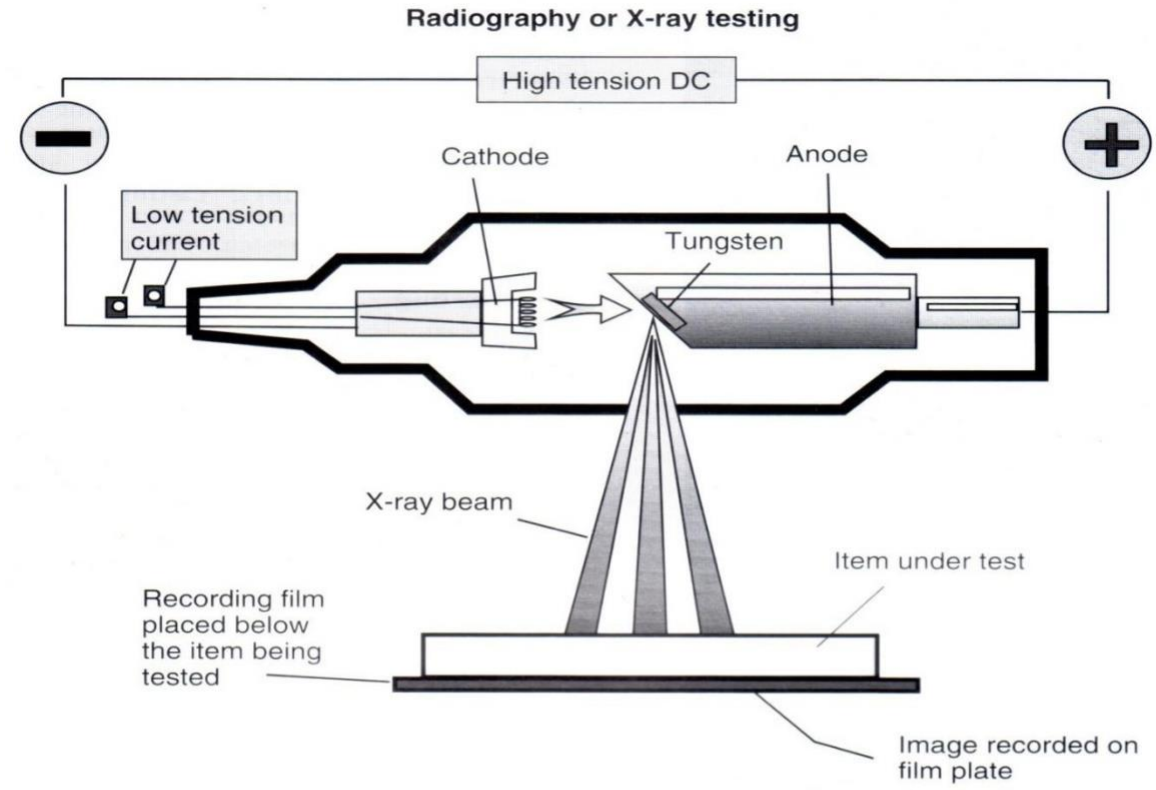
Radiography or X-ray testing
High tension DC
Cathode
Anode
Low tension current
Tungsten
X-ray beam
Item under test
Recording film placed below the item being tested
Image recorded on film plate

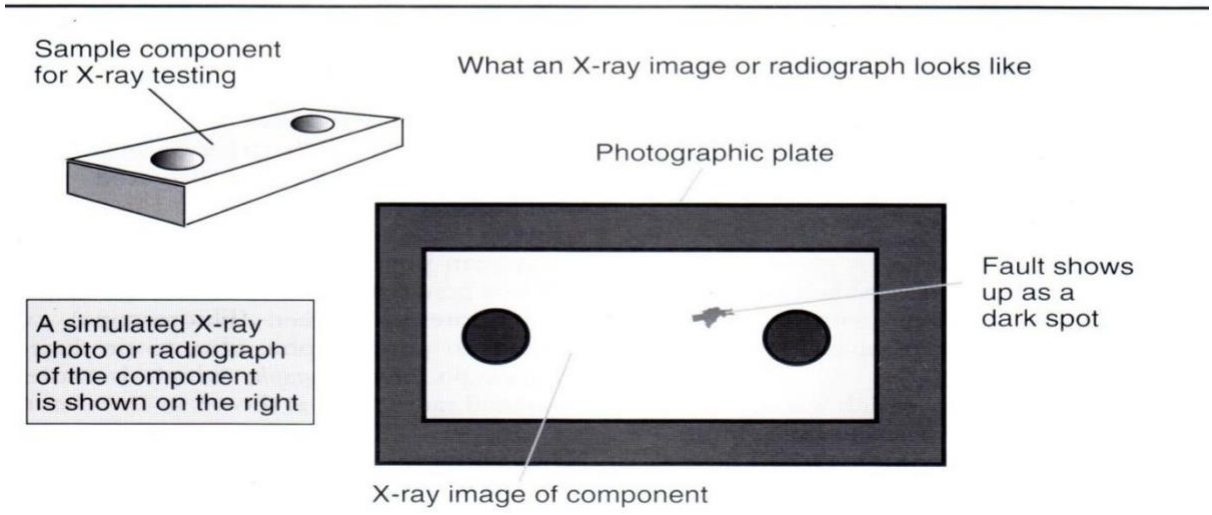
Sample component for X-ray testing
What an X-ray image or radiograph looks like
Photographic plate
Fault shows up as a dark spot
A simulated X-ray photo or radiograph of the component is shown on the right
X-ray image of component